AD-A034 174 INTERNATIONAL NICKEL CO INC SUFFERN N Y PAUL D MERICA--ETC F/G 11/6
OXIDE DISPERSION STRENGTHENED HIGH VOLUME FRACTION GAMMA PRIME --ETC(U)
DEC 76 L R CURWICK N00019-75-C-0313
UNCLASSIFIED 2218.4 NL

1 OF 1
AD A034174

END
DATE FILMED
2-77

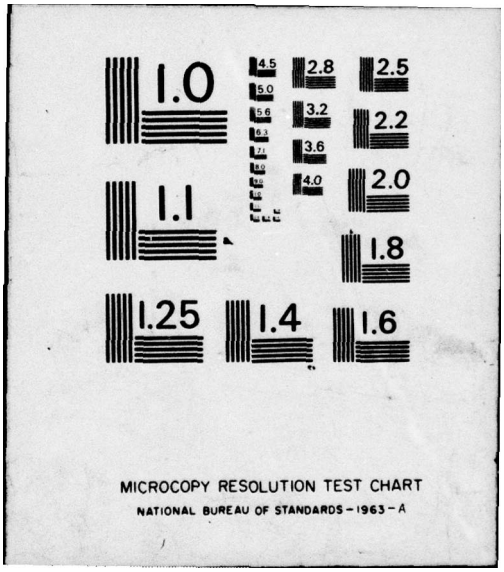
1.0
1.1
1.25
1.4
1.6
1.8
2.0
2.2
2.5
2.8
3.2
3.6
4.0
4.5
5.0
5.6
6.3
7.1
8.0
MICROCOPY RESOLUTION TEST CHART
NATIONAL BUREAU OF STANDARDS-1963-A

THE INTERNATIONAL NICKEL COMPANY, INC.
PAUL D. MERICA RESEARCH LABORATORY
STERLING FOREST
SUFFERN, NY 10901

(14) PROJECT REPORT 2218.4

(6) OXIDE DISPERSION STRENGTHENED HIGH VOLUME FRACTION GAMMA PRIME Ni-Cr-Al ALLOYS MADE BY MECHANICAL ALLOYING.

(9) FINAL REPORT, May 75-Sep 76,
(15) Contract N00019-75-C-0313

(11) DECEMBER 1976

(12) 75p.

Reported by LeRoy R. Curwick

(10) LeRoy R. Curwick
Research Metallurgist
Nickel Alloys Section

Approved by J.S. Benjamin

J.S. Benjamin
Research Manager
Materials Research Group

409 994

UNCLASSIFIED

SECURITY CLASSIFICATION OF THIS PAGE (When Data Entered)

REPORT DOCUMENTATION PAGE		READ INSTRUCTIONS BEFORE COMPLETING FORM
1. REPORT NUMBER	2. GOVT ACCESSION NO.	3. RECIPIENT'S CATALOG NUMBER
4. TITLE (and Subtitle) OXIDE DISPERSION STRENGTHENED HIGH VOLUME FRACTION GAMMA PRIME Ni-Cr-Al ALLOYS MADE BY MECHANICAL ALLOYING ✓		5. TYPE OF REPORT & PERIOD COVERED FINAL REPORT MAY, 1975-SEPT. 1976
		6. PERFORMING ORG. REPORT NUMBER
7. AUTHOR(s) L.R. CURWICK		8. CONTRACT OR GRANT NUMBER(s) N00019-75-C-0313 NEW
9. PERFORMING ORGANIZATION NAME AND ADDRESS THE INTERNATIONAL NICKEL COMPANY, INC. PAUL D. MERICA RESEARCH LABORATORY STERLING FOREST, SUFFERN, NY 10901		10. PROGRAM ELEMENT, PROJECT, TASK AREA & WORK UNIT NUMBERS
11. CONTROLLING OFFICE NAME AND ADDRESS NAVAL AIR SYSTEMS COMMAND DEPARTMENT OF THE NAVY WASHINGTON, DC 20361		12. REPORT DATE DECEMBER, 1976
		13. NUMBER OF PAGES
14. MONITORING AGENCY NAME & ADDRESS(if different from Controlling Office)		15. SECURITY CLASS. (of this report) UNCLASSIFIED
		15a. DECLASSIFICATION/DOWNGRADING SCHEDULE

16. DISTRIBUTION STATEMENT (of this Report)

"APPROVED FOR PUBLIC RELEASE - DISTRIBUTION UNLIMITED"

17. DISTRIBUTION STATEMENT (of the abstract entered in Block 20, if different from Report)

18. SUPPLEMENTARY NOTES

19. KEY WORDS (Continue on reverse side if necessary and identify by block number)

OXIDE DISPERSION STRENGTHENED
MECHANICAL ALLOYING
GAMMA PRIME
NICKEL-BASE SUPERALLOYS
ZONE ANNEALING

GAMMA PRIME

20. ABSTRACT (Continue on reverse side if necessary and identify by block number)

An investigation was conducted to determine the feasibility of producing oxide dispersion strengthened high volume fraction (γ') Ni-Cr-Al alloys by mechanical alloying. The objective of this work was to develop ODS alloys which would derive a significant high temperature strength increment from the retention of high volume fractions (>50%) of (γ') at their intended use temperature of 2000°F. In addition, higher aluminum, (β) phase containing alloys were investigated, as well

GREATER THAN

BETA

DD FORM 1 JAN 73 1473 EDITION OF 1 NOV 65 IS OBSOLETE

SECURITY CLASSIFICATION OF THIS PAGE (When Data Entered)

as quaternary additions of Ti and W to a high volume fraction γ' (GAMMA PRIME) base alloy.

This study showed that it is possible to produce a highly directionally recrystallized structure in these high volume fraction (90-97%) γ' alloys. However, the best structure and hence the highest strength was obtained in the lower (90% vs. 97%) volume fraction γ' alloy. Titanium was found to be detrimental to the structural response of quaternary Ni-Cr-Al-Ti ODS alloys. Tungsten additions resulted in significantly improved high temperature strengths. On a density corrected basis the 1000 hour specific rupture strength of a Ni-Cr-Al-W ODS alloy surpassed that of DS Mar M-200 (above 1530°F) and certain current DS γ/γ'-α eutectic alloys (above 1630°F). Tensile, intermediate temperature stress rupture, and corrosion resistant properties were also determined.

An attempt to produce β phase precipitation hardened ODS Ni-Cr-Al alloys by mechanical alloying was unsuccessful.

OXIDE DISPERSION STRENGTHENED HIGH VOLUME FRACTION GAMMA PRIME Ni-Cr-Al ALLOYS MADE BY MECHANICAL ALLOYING

TABLE OF CONTENTS

I. INTRODUCTION

Today, several distinct types of directional structures offer potential for increased operating temperatures (100-350°F) for gas turbine vanes and blades. Among these are the oxide dispersion strengthened (ODS) alloys(1-3) produced by mechanical alloying(4). The ODS + γ' nickel-base superalloys which have been produced to date offer substantial increases in temperature capability as shown in Figure 1.

In these previous ODS alloy investigations, alloys with low incipient melting points, conventional volume fractions of γ' (30-70%), and low γ' solvus temperatures were studied. At intermediate temperatures (1400°F) the ODS + γ' alloys enjoy a significant strength increment over their γ' free counterparts; e.g., TD-Ni and TD-Ni-Cr. As the use temperatures are raised and the γ' solvus is approached, the γ' volume fractions decrease significantly and the γ' strengthening increment decreases to zero. This occurs at approximately 1600-1800°F for present ODS + γ' alloys. In this research program alloys were developed with very high volume fractions of γ' at the intended use temperature of 2000°F. The expected γ' strengthening increment combining with the ODS effect should result in higher 2000°F strength.

This report describes work done under NAVAL AIR SYSTEMS COMMAND Contract No. N00019-75-C-0313 to develop ODS nickel-base superalloys with 80-90% γ' for turbine blades operable at 2000°F and higher. The work was planned and carried out in two phases. In Phase I, the feasibility of producing high volume % γ' Ni-Cr-Al ODS alloys by mechanical alloying was determined. Phase II was planned to explore ternary Ni-Cr-Al alloys in the γ/β, γ'/β and $\gamma/\gamma'/\beta$ phase fields. In addition several quaternary alloys of the Ni-Cr-Al-Ti and Ni-Cr-Al-W systems were studied.

II. EXPERIMENTAL PROCEDURES

2.1 Alloy Selection

Two ternary Ni-Cr-Al alloys were selected for investigation in Phase I. The compositions given in Table I correspond to 20 and 17.5 atomic % Al, 10 atomic % Cr, Ni-Cr-Al alloys, respectively.

As shown in the 2100°F ternary diagram of Figure 2, alloy 1 lies within the γ/γ' phase field at this temperature, while alloy 2 lies in the γ field. Thus, alloy 1 should retain significantly more γ' at 2100°F. These alloys were selected in an attempt to determine the effectiveness of γ' strengthening in these ODS alloys at high temperature.

In Phase II five ternary alloy compositions were selected from the $\gamma/\gamma'/\beta$, γ'/β and γ/β phase fields of the Ni-Cr-Al system. The objective of Phase II was to determine the feasibility of producing β phase precipitation hardening in a simple ODS + γ' alloy. In addition, four high volume % γ' ODS alloys, with quaternary additions of Ti or W, were produced in Phase II. These alloy compositions are also given in Table I.

2.2 Attritor Processing

The following powders were used for mechanical alloying:

Nickel Powder Type 123
Elemental Chromium
Elemental Tungsten
Ni-46Al Master Alloy
Ni-28Ti-17Al Master Alloy
Y_2O_3 (Calcined Yttrium Oxalate)

Powder batches of the selected compositions were mechanically alloyed in attrition mills under controlled conditions which were established by Inco outside the scope of this contract. The resultant mechanically alloyed powder was characterized using chemical analysis for O, N, C and Fe, screen analysis, and metallographic examination. The criteria for accepting powder as well processed are outlined in Reference 4. Basically one looks for a completely homogeneous processed powder when examined metallographically. Experience has taught that a coarse powder size distribution, and normal oxygen ($\sim$.5-.8 wt. %) and iron (.5-.8 wt. %) levels are indicative of well processed powder.

2.3 Extrusion

After screening to remove the coarse +12 mesh particles, powder batches of each composition were cone blended for two hours and packed into 3.5 inch OD steel extrusion cans. Between six and nine cans were prepared for each of the six compositions investigated in this program. The extrusion cans were sealed in air prior to extrusion.

Extrusions were made after preheating the billets two hours to temperatures ranging from 1750 to 2200°F. Round extrusion dies were used yielding ratios ranging from 12 to 55:1. Conical dies having an included angle of 90° were employed. Lubrication was provided by a glass pad on the die face with oil in the extrusion chamber and a glass wrap on the billet.

All extrusions were performed on a 750 ton Loewy Hydropress at throttle settings of 30 or 100%. Ram speed and pressure were continuously recorded during each extrusion. Occasional recorder malfunction resulted in no record for three of the fifty extrusions made in this work.

2.4 Heat Treatment

The objective of the extrusion studies was to determine the conditions required to yield a coarse elongated grain structure in each alloy, upon heat treatment. The necessity of obtaining this structure to achieve maximum high temperature strength in ODS alloys is well documented(5,6).

The recrystallization response of an extruded bar was determined by selected isothermal or stationary gradient annealing heat treatments. In Phase I isothermal anneals at 2250, 2300, 2350 and 2400°F for 1/2 hour were used to determine the recrystallization response of alloy 1 and 2 extrusions. These samples were sectioned parallel to the extrusion direction to reveal the longitudinal nature of the recrystallized grains, etched, and examined metallographically.

In Phase II stationary gradient anneals were used to determine the recrystallization behavior as a function of annealing temperature. Four inch long extruded bar samples were individually annealed in a gradient furnace having the thermal profile shown in Figure 3. Total annealing time was 1/2 hour. After heat treatment these bars were surface ground parallel to the extrusion direction to reveal the recrystallized grain structure as a function of position along the gradient. This is a simple method for determining the temperature range over which recrystallization to a coarse grain structure will take place. It also pinpoints the critical heat treatment temperature at which the best coarse elongated grain structure is achieved.

Zone annealing can be an effective way of increasing the grain aspect ratio, and hence the high temperature strength, of ODS superalloys(1,7). Generally, extruded bar which shows a coarse grain structure (elongated or equiaxed) on isothermal or static gradient annealing, will respond favorably to zone annealing. Selected bars were zone annealed in the same gradient furnace (Figure 3) at 5.3 inches per hour and maximum zone temperatures ranging from 2260 to 2400°F. Specimens were cut from these zone annealed bars and sectioned to reveal the grain aspect ratio achieved.

A heat treatment study was conducted to determine the volume % γ' in the Ni-Cr-Al alloys 1 and 2 and in the Ni-Cr-Al-W alloys 7 and 8.

2.5 Mechanical Testing

Specimens for mechanical testing were ground from round heat treated bars with their tensile axis oriented parallel to the extrusion direction. In all cases this corresponded to the direction of structural elongation. Stress rupture tests were performed at 1400, 2000, and 2100°F in air. Initially 24 hour/2 ksi step loading was used to determine the capability of the material. Constant load tests at 1400, 2000 and 2100°F and at several different loads were used to determine the stress/temperature/life capability of alloys 1, 2, 7 and 8 material with the best grain structure achieved in this program. These tests were performed in accordance with the appropriate ASTM specification on specimens with .125 inch gauge diameter, gauge length of 1 inch, and .25 inch -20NC threaded ends. Elongation and reduction of area were measured from the fractured specimens.

Creep tests were run on alloy 2 specimens at 1400 and 2000°F in air. Extensometer arms were attached to the threaded ends of the test specimens. These tests were run on specimens identical in dimension and method of manufacture to those used for stress rupture testing. Extension across the threaded ends was measured throughout the test. Elongation and reduction of area were measured on the fractured specimen.

Tensile testing on selected alloy bars was performed at room temperature and 1400°F in air. Again the test specimens were identical in dimension, orientation, and method of manufacture to those used for stress rupture and creep testing. Only specimens of alloy 2 were tensile tested.

2.6 Physical and Chemical Testing

Density measurements were made by simple calculations based on the dimensions and weight of cylindrical oxidation test specimen. This method is accurate to within 1%.

Oxidation tests were performed at 2000°F for 504 hours. The test was cyclic in nature with the specimens being cooled rapidly to room temperature and weighed daily. The environment was low velocity air + 5% H_2O. After final weight measurements the samples were descaled by a light Al_2O_3 grit blast and final weight loss was measured.

Burner rig sulfidation tests were conducted at 1700°F for 168 hours. The rig used corresponds to the G.E. Lynn low velocity burner rig(8). This test ran on a one hour cycle, 58 minutes rotating in the flame, two minutes in air blast. The flame conditions were a 30:1 air + 5 ppm seawater (ASTM Spec. D1141-52) to fuel (.3% sulfur JP-5) ratio at low velocity. The specimens were weighed each 24 hours and standard diametric (cross section) metal loss and grain boundary penetration measurements were made at the end of the test. Descaled weight loss was also determined.

A [100] texture in directional structures is known to provide a definite advantage in thermal fatigue resistance. A low elastic modulus was observed on one alloy 2 extruded and zone annealed bar. X-ray diffraction texture analysis was used to determine preferred orientations of the directional structure observed in alloy 2 bars with high and low elastic moduli.

III. RESULTS AND DISCUSSION

3.1 Mechanically Alloyed Powder Production

In Phase I, alloy 1 powders were initially mechanically alloyed in a small attritor mill producing 9.35 lbs. of powder per batch. Nine batches were produced in this mill. Batches V1, V2 and V3 were preliminary runs used to adjust attritor processing conditions. When well processed powder was achieved, six additional heats were produced. Characterization of these first nine batches of alloy 1 powder is given in Table II. Metallographic examination showed that batches V1 and V2 were grossly underprocessed (shown in Figure 4). The remaining batches were essentially well processed but with minor inhomogeneities. This is illustrated in Figure 5 for batch V4.

Because of the processing experience with alloy 1, alloy 2 was processed in a larger attritor yielding 18.7 lbs. of powder per batch. A wash batch and four additional batches were produced. All showed excellent processing as shown for batch V12 in Figure 6. Powder characterization for these alloy 2 batches is also given in Table II.

Additional powder batches were produced of alloy 1 in the larger attritor. As with alloy 2, a wash heat and four powder batches were produced. All showed excellent processing as given in Table II and Figure 7. This second series was produced primarily due to the poor extrusion response demonstrated by the initial powder produced in the smaller attritor.

In Phase II three composition series were produced. The first of these included alloys 3 and 4 of Table I. Alloy 3 is a Ni-Cr-Al alloy whose composition lies within the $\gamma' + \beta$ phase field of Figure 2. Alloy 4 lies within the $\gamma + \gamma' + \beta$ phase field. Four attempts were made to produce these alloys by mechanical alloying. The character of the powder produced is shown in Table III. In all cases the powder showed no signs of welding and coarsening as is desirable. Due to the extreme grinding regime encountered, these powders suffered from high iron pickup (from the milling medium). In addition several of the powder batches were pyrophoric and picked up high oxygen levels when exposed to air. Because of the difficulty encountered in producing the β phase containing Ni-Cr-Al alloys the work was redirected toward more profitable alloy development work. Two additional series of alloys were made, alloys 5 and 6 were made with Ti additions and alloys 7 and 8 with W additions to a Ni-Cr-Al base.

Three powder batches were made of each alloy 5, 6, 7 and 8 in the larger attritor mill. In each case a wash

batch was produced and discarded followed by two additional batches of each composition. Powder characterization data on these last four alloys are given in Table IV. In all cases excellent powder processing was achieved. Figures 8 to 11 show powder micros for each alloy.

3.2 Extrusion

Alloy 1 powder batches V4 through V9 were cone blended and the resultant powder batch was designated V10. This powder was packed into nine mild steel cans and extruded at the conditions shown in Table V. Also shown in Table V are the extrusion conditions for the second alloy 1 powder batch V22 (blend of V17-V20) and alloy 2 powder batch V21 (blend of V12-V15). In the extrusion work on the alloy 1 and 2 powders the throttle setting was fixed at 100% with extrusion speeds ranging from 2.0 to 9.4 in/sec.

Six cans each were extruded of alloys 5, 6, 7 and 8 powders. The extrusion conditions and recorded extrusion speeds are given in Table VI. For these alloys an attempt was made to include extrusion speed as a controlled variable by varying the extrusion press throttle setting. In this case speed variations from 2.0 to 14.9 in/sec were obtained.

3.3 Heat Treatment - Recrystallization Response

The objective of the extrusion work was to determine the conditions required to yield a coarse elongated grain structure in these materials, upon heat treatment. The necessity of obtaining this highly directional structure to achieve maximum high temperature strength in ODS alloys is well known. The nature of the recrystallization response is generally described in terms of transverse grain diameter (fine .1-1μm, medium 1-50μm and coarse 50-250μm), and grain aspect ratio (length/diameter). For optimum high temperature strength, a coarse grain size with a grain aspect ratio (GAR) of about 10 is required.

The isothermal annealing recrystallization response of alloys 1 and 2 extruded bar samples is described in Table VII. As can be seen the first series of alloy 1 extrusions, V10A-V10I did not respond favorably. The second series of alloy 1 extrusions V22A-V22H showed a more favorable recrystallization response, however, the ideal coarse elongated grain structure was not achieved. Alloy 2 responded better, with high grain aspect ratios achieved for several extrusion conditions. Typical grain structures achieved from alloy 1, V22 extrusion and alloy 2, V21 extrusions are shown in Figures 12 and 13, respectively. A map of isothermal recrystallization response vs. extrusion conditions are shown in Figures 14 and 15 for alloys 1 and 2 respectively. These maps show that both alloys exhibit better recrystallization response at high extrusion temperature and ratio.

Based on their favorable isothermal recrystallization response most of the alloy 2 extrusions and three of the alloy 1 extrusions were zone annealed to improve grain aspect ratio. As-extruded 12.5 in. long rods were zone annealed at maximum zone temperatures of approximately 2350°F at a speed of 5.3 in/hr. The response of these bars to zone annealing is shown in Table VII. A more elongated grain structure was achieved in several cases. Although grain aspect ratios greater than 10:1 were achieved in one alloy 2 bar, the best GAR achieved in alloy 1 was 6.5:1. An example of the dramatic effect that can be achieved through zone annealing is shown in Figure 16.

The recrystallization response of the alloy 5-8 extruded bars was studied using static gradient annealing. As described earlier 4 in. long rods from each extruded bar were individually annealed in a gradient ranging from about 2400°F down to 1550°F. In all cases the temperature profile along the rod was approximately the same as that shown in Figure 3.

The gradient annealing results for the Ti-containing alloys 5 and 6 are shown in Figures 17 and 18 respectively. These figures show macrographs of gradient annealed specimens from alloy 5 extrusions V31A-F and alloy 6 extrusions V33A-F. These results show that recrystallization was incomplete in all cases.

The gradient annealing results for the W-containing alloys 7 and 8 are shown in Figures 19 and 20 respectively. In both cases a coarse elongated grain structure was achieved at two or three extrusion conditions.

Based on the gradient annealing response one alloy 7 bar, V35D, and two alloy 8 bars, V37D and V37-F were zone annealed using maximum zone temperatures of 2280°F and a zone speed of 5.3 in/hr. Figures 21-23 show the zone annealed grain structure achieved with these three bars.

3.4 γ' Volume Fraction

A heat treatment study was conducted to determine the volume % γ' in alloys 1 and 2. The γ' determinations were made using replica electron microscopy at 4,900 and 11,500X followed by quantitative metallography. The heat treatments used and volume % γ' observed are given in Table VIII. Figures 24 and 25 showed the γ' size, shape and distribution in alloys 1 and 2. Note that at 2100°F both alloys retain a significant volume fraction of γ'.

Figures 26 and 27 show the γ' size, shape and distribution in alloys 7 and 8 after furnace cooling to room temperature when zone annealing. Table VIII shows the volume % γ' in these alloys as determined using quantitative metallography. Note that in these alloys the γ' volume % decreases as W is substituted for Ni in the alloy 2 base.

3.5 Stress Rupture and Creep Rupture

The 2000°F stress rupture properties of alloy 1 extruded and heat treated bar was determined by step loading or constant loading tests. The results of thse tests on conventionally heat treated bar and zone annealed bar from alloy 1 extrusions V22A-D are given in Table IX. None of the alloy 1 bars showed good 2000°F properties despite the achievement of reasonably good grain aspect ratios. Since extruded bars V22E-H did not show further structural improvements no testing was done on those bars.

Results of 2000°F stress rupture tests on conventionally annealed alloy 2 extruded bars are given in Table X. These properties are consistently better than those achieved in alloy 1. Zone annealing of select alloy 2 bars resulted in significant improvements in GAR and 2000°F stress rupture properties. These are given in Table XI.

Figure 28 shows a 2000°F rupture stress vs. rupture life plot for alloy 1 bar V22D and alloy 2 bar V21G compared with an earlier Inco development alloy, MA 755E. This plot shows that alloy 2 bar with the desired coarse elongated grain structure has 2000°F strength slightly better than MA 755E. Since this grain structure was not achieved in the alloy 1 bars, the high temperature strength was considerably lower. For this reason no further mechanical testing was done on the alloy 1 material.

Zone annealed bars of alloy 2 were tested at 1400, 2000 and 2100°F in stress rupture to obtain sufficient data to generate a stress vs. temperature plot for comparison with competitive alloys. Results of these tests are given in Table XII. In addition several heat treatments were applied to zone annealed bar from extrusion V21G to determine whether improvements in 1400°F creep behavior were possible. The results of these 1400°F creep tests are given in Table XIII and creep curves are plotted in Figure 29. Significant improvements in 1400°F rupture life and creep ductility were observed. A creep test was also conducted at 2000°F and is shown in Figure 30. Properly heat treated alloy 2 shows excellent creep behavior at both 1400 and 2000°F. The excellent ductility achieved in the simple alloy is very encouraging.

Alloys 7 and 8 were tested in stress rupture at 1400, 2000 and 2100°F. Results of the 1400°F tests are given in Table XIV and the high temperature test results are combined in Table XV. At 1400°F alloy 7 (3.4 wt. % W) bar V35D is slightly stronger at 100 hours than alloy 8 (6.7 wt. % W) bar V37D. This is illustrated in Figure 31. However, this difference may be attributed to a slightly finer grain diameter for bar V35D.. At 2000 and 2100°F, alloy 8 bar V37F is demonstrably stronger than alloy 7 bar V35D. This is illustrated in Figure 32. Both bars have extremely elongated grain structures. Therefore, the strength increment achieved may be attributed to the effect of solid solution strengthening at these temperatures. When the alloy 7 and 8 results are compared to alloy 2 a significant increase in high temperature strength has been achieved.

The high temperature strength capability of the high volume % γ' ODS alloys developed in this work is summarized in Figure 33. This figure is a density corrected specific stress rupture strength vs. T °F plot for 1000 hours for alloy 8 compared to two competitive alloy systems. Because the density of a material exerts a strong influence on the tensile stress in a rotating turbine blade, the stress rupture strength of these alloys have been normalized with respect to alloy density to the first power. Density data for these alloys is given in Table XVI. Note there is only a small density increase for alloy 7.

Figure 33 compares the simple Ni-Cr-Al-W ODS alloy 8 with a directionally solidified conventional nickel-base superalloy and a current directionally solidified $\gamma/\gamma'-\alpha$ eutectic alloy(9). This figure shows that the 1000 hour density corrected specific rupture strength capability of alloy 8 surpasses DS Mar M-200 + Hf above 1530°F and a current DS $\gamma/\gamma'-\alpha$ eutectic alloy above 1630°F. Below these crossover temperatures the ODS alloy is not as strong as the DS alloys.

3.6 Tensile Testing

Alloy 2 bars were tested in tension at room temperature and 1400°F after various heat treatments. The results of these tests are given in Table XVII. For comparison tensile test data for the conventional cast alloy Mar M-200 is included. These results show that given an appropriate heat treatment alloy 2 has tensile properties equivalent to the widely used cast nickel-base superalloys; e.g., IN-100, Mar M-200, and IN-792.

An interesting observation was made concerning the room temperature modulus of alloy 2 bar V21G. The extremely low elastic modulus observed, $\sim 21 \times 10^6$ psi, indicated that this

bar had recrystallized to a [100] texture. This was confirmed by x-ray texture analysis. The [100] texture is desirable for turbine blade and vane alloys where thermal expansion and thermal fatigue problems may be reduced. Alloy 2 bar V21H did not show the low modulus and x-ray analysis revealed a [112] texture was present in this bar. These results show that although alloy 2 is capable of yielding a [100] texture, the extrusion and possibly the heat treatment conditions are critical variables.

3.7 Hot Corrosion and Oxidation

Due to time limitation on this work only alloys 1 and 2 were tested for hot corrosion and oxidation resistance. Hot corrosion tests were conducted in a low velocity burner rig of the GE-Lynn type. Both alloys were tested and compared with conventional superalloys and MA 755E. The burner rig tests were conducted at 1700°F over 168 hours with hourly cycles to room temperature. The flame composition is produced by burning JP-5 fuel (.3% sulfur) at a fuel-to-air ratio of 30:1. The air is injected with 5 ppm seawater (ASTM Spec. D1141-52). The results of this test are given in Table XVIII. The alloy 2 sample was essentially destroyed after 168 hours. Although the alloy has sulfidation resistance superior to alloy 713C and IN-100 it is not adequate when compared with IN-738 and MA 755E. The higher Al-containing alloy 1 does show improved hot corrosion resistance. However, increasing the aluminum content for improved sulfidation cannot be seriously considered due to processing limitations.

High temperature cyclic oxidation tests were conducted on duplicate samples of alloy 2. These were performed at 2012°F for 504 hours with daily cycles to room temperature. The atmosphere was air-5% water vapor at low velocity (15 in^3/min). Results of these tests given in Table XIX, show that this alloy has excellent oxidation resistance. The descaled weight loss for this alloy is less than observed for IN-100 and far less than that observed for alloy 713C, IN-738 and MA 755E. The extremely high oxidation resistance exhibited by the Ni-10Cr-9Al-1.1Y_2O_3 alloy 2 makes it ideally suited for high temperature turbine blade applications.

IV. CONCLUSION

This work has shown that it is possible to produce oxide dispersion strengthened high volume fraction γ' (90-97%) Ni-Cr-Al alloys by mechanical alloying. However, it was found that at the highest γ' level thermomechanical processing and recrystallization response decreased. Because a more elongated grain structure was obtained in the alloy with the lower (90%) γ' volume fraction significantly better high temperature strength was achieved. For this reason it was not possible to directly measure the effect of γ' volume fraction on the high temperature rupture strength in these alloys.

Through quaternary alloy additions of tungsten to the alloy 2 base composition further improvements in high temperature strength were achieved. Despite a small increase in density the high tungsten alloy 8 showed superior 1000 hour density corrected specific rupture strength when compared to DS Mar M-200 (above 1530°F) and a current DS γ/γ'-α eutectic alloy (above 1630°F).

An investigation of quaternary titanium additions to the alloy 2 base composition showed that this element is detrimental to thermomechanical processing and recrystallization response. At a level of 2.8 wt. % only limited recrystallization was observed. Therefore, except in small quantities (<2.5 wt. %), titanium cannot be used as a γ' strengthener in these alloys.

In addition to excellent high temperature properties the simple ODS high volume fraction γ' alloys developed in this work show a promising range of other important mechanical and physical properties. Alloys 2, 7 and 8 show 1400°F/1000 hour rupture strength >713C. Alloy 2 has tensile properties equivalent to cast Mar M-200 and greater than IN-100. In addition it has been determined that it is possible to achieve a [100] texture in alloy 2 bar although control of thermomechanical processing variables is critical.

In view of the significant improvements in properties achieved by modest quaternary tungsten additions, further alloy developments should be pursued.

ACKNOWLEDGEMENT

The author gratefully acknowledges the technical assistance of Kenneth Andryszak and the support of all PDMRL personnel in this work.

REFERENCES

1. Cairns, R.L., Curwick, L.R., and Benjamin, J.S., "Grain Growth in Dispersion Strengthened Superalloys by Moving Zone Heat Treatments", Metallurgical Transactions, Vol. 6A, Jan. 1975, pp. 179-188.

2. Glasgow, T.K. and Quatinetz, M., "Preliminary Study of Oxide-Dispersion-Strengthened B-1900 Prepared by Mechanical Alloying", NASA TM X-3303, Oct. 1975.

3. Glasgow, T.K., "An Oxide Dispersion Strengthened Ni-W-Al Alloy with Superior High Temperature Strength", Proceedings of the Third International Symposium on Superalloys: Metallurgy and Manufacture, Sept. 1976, pp. 385-394.

4. Benjamin, J.S., "Dispersion Strengthened Superalloys by Mechanical Alloying", Metallurgical Transactions, Vol. 1, Oct. 1970, pp. 2943-2951.

5. Ansell, G.S. and Weertman, J., "Creep of a Dispersion Hardened Aluminum Alloy", Transactions TMS-AIME, Vol. 215, Oct. 1959, pp. 838-843.

6. Wilcox, B.A. and Clauer, A.H., "The Role of Grain Size and Shape in Strengthening of Dispersion Hardened Nickel Alloys", Acta Metallurgica, Vol. 20, No. 5, Mar. 1972, pp. 743-757.

7. Allen, R.E., "Directionally Recrystallized TD Ni Cr", Proceedings of the Second International Symposium on Superalloys, Sept. 1972, pp. X1-X22.

8. Bergman, P.A., Sims, C.T., and Beltran, A.N., "Development of Hot-Corrosion-Resistant Alloys for Marine Gas Turbine Service", ASTM STP 421, Am. Soc. Testing Mat'ls., 1967, p. 43.

9. Lemkey, F.D., "Development of Directionally Solidified Eutectic Nickel and Cobalt Alloys", Final Report, Contract No. N62269-35-C-0129, Naval Air Systems Command, Dec. 1975, Figure 26.

TABLE I

COMPOSITIONS OF TERNARY AND QUATERNARY ALLOYS

Alloy No.	Composition, Wt. %						Applicable Phase Fields*
	Ni	Cr	Al	Ti	W	Y_2O_3	
1	79.5	10.1	10.4	--	--	1.1	$\gamma + \gamma'$
2	81.1	9.9	9.0	--	--	1.1	γ
3	79.8	6.2	14.0	--	--	1.1	$\beta + \gamma'$
4	78.6	8.3	13.1	--	--	1.1	$\beta + \gamma + \gamma'$
5	80.8	9.7	6.8	2.8	--	1.1	$\gamma + \gamma'$
6	79.8	9.6	5.2	5.3	--	1.1	$\gamma + \gamma'$
7	78.1	9.7	8.8	--	3.4	1.1	γ
8	75.3	9.5	8.6	--	6.7	1.1	γ

*At 2100°F (1150°C)

TABLE II

POWDER CHARACTERIZATION OF ALLOY 1 POWDER BATCHES V1-V9; ALLOY 2 POWDER BATCHES V11-V15; AND ALLOY 1 POWDER BATCHES V16-V20

Batch No.	Chemistry, Wt.%				Screen Analysis, Mesh Size %							
	O	N	C	Fe	+40	-40/+80	-80/+100	-100/+140	-140/+200	-200/+230	-230/+325	-325
V1	.59	.031	.068	1.4	ND	-	-	-	-	-	-	-
V2	.43	.030	.051	.60	9.8	32.1	8.5	11.7	13.3	5.2	6.9	12.5
V3	.46	.030	.046	.33	ND	-	-	-	-	-	-	-
V4	.52	.035	.041	.37	18.8	37.5	9.1	11.6	10.8	2.8	4.3	5.1
V5	.51	.033	.047	.35	20.2	38.6	8.6	11.4	10.5	3.1	3.5	4.1
V6	.50	.036	.043	.32	19.5	36.7	10.4	11.9	10.8	3.5	3.8	3.4
V7	.47	.034	.041	.34	24.5	34.5	7.8	10.0	9.5	3.4	4.8	5.5
V8	.55	.032	.043	.25	18.2	34.8	9.2	12.2	10.3	3.5	4.4	7.4
V9*	.52	.030	.041	.22	19.7	41.5	10.6	11.4	7.8	1.8	3.3	3.9
V11	.70	.055	.045	.62	12.7	42.8	11.3	14.2	11.0	2.4	2.7	2.9
V12	.79	.047	.044	.55	16.5	33.7	10.3	15.5	11.9	3.3	4.0	4.8
V13	.63	.046	.043	.46	20.9	51.8	10.3	9.7	4.1	0.4	1.4	1.4
V14	.64	.052	.045	.39	19.6	47.1	9.2	9.2	8.5	1.2	2.1	3.1
V15	.86	.052	.046	.36	14.6	45.5	9.1	11.3	9.7	2.3	3.6	3.9
V16	.79	.049	.042	.30	15.9	39.9	9.1	11.4	10.4	3.5	4.3	5.5
V17	.72	.038	.041	.33	20.3	50.2	8.2	7.3	5.5	1.5	2.6	4.4
V18	.71	.034	.042	.33	5.2	37.5	13.7	13.7	12.8	3.6	5.4	8.1
V19	.74	.044	.049	.29	11.2	36.9	10.2	12.2	12.4	3.7	5.6	7.8
V20+	.70	.037	.044	.32	31.8	48.9	5.6	5.4	4.4	0.9	1.4	1.6

* The batch numbered V10 was applied to the total of the combined Alloy 1 batches V4-V9 which were cone blended.

\+ Batch V21 refers to the combination of Alloy 2 batches V12-V15 and Batch V22 refers to the combination of Alloy 1 batches V17-V20.

ND Not Determined

TABLE III

POWDER CHARACTERIZATION OF ALLOY 3 AND 4 POWDER BATCHES V-23-26

Batch No.	Chemistry Wt.%				Screen Analysis, Mesh Size %							
	O	N	C	Fe	+40	-40/+80	-80/+100	-100/+140	-140/+200	-200/+230	-230/+325	-325
V-23	.71	.053	.057	4.3	0.3	0.5	0.2	0.7	1.1	0.2	1.6	95.4
V-24	1.40	.082	.066	4.4	-	-	-	-	-	-	-	>90
V-25	4.53	.13	.13	9.2	-	-	-	-	-	-	-	>90
V-26	4.60	.14	.14	9.8	-	-	-	-	-	-	-	>90

TABLE IV

POWDER CHARACTERIZATION OF ALLOY 5, 6, 7 AND 8 POWDER BATCHES V-31-38

Batch No.	O	N	C	Fe	+40	-40/+80	-80/+100	-100/+140	-140/+200	-200/+230	-230/+325	-325
V31*	.63	.097	.063	.57	17.3	52.1	10.1	8.5	6.6	1.5	1.6	2.3
V32	.65	.089	.062	.54	20.4	41.3	8.1	11.6	10.8	2.8	2.7	2.3
V33	.72	.082	.061	.55	19.6	53.4	9.7	9.4	4.5	1.0	1.2	1.2
V34	.74	.097	.061	.52	12.2	49.4	11.6	12.8	9.6	1.6	1.7	1.1
V35	.66	.056	.063	.45	18.1	48.5	8.1	8.1	8.7	2.5	3.1	2.9
V36	.68	.064	.056	.47	21.5	55.6	6.7	6.6	5.2	1.1	1.7	1.6
V37	.56	.063	.057	.51	15.0	44.6	9.5	11.4	10.2	2.7	3.4	3.2
V38	.52	.054	.051	.36	13.9	52.5	11.3	11.3	7.3	1.2	1.4	1.1

* The batch number V31 was assigned to the total of the combined alloy 5 batches V31 and V32 which were cone blended. Likewise, V33, V35, and V37 were assigned to the two cone blended batches of alloys 6, 7 and 8 respectively.

TABLE V

EXTRUSION CONDITIONS FOR ALLOY 1, BLENDED BATCH V10; ALLOY 2, BLENDED BATCH V21; AND ALLOY 1, BLENDED BATCH V22

Billet No.	Temp., °F(°C)	Ratio	+Speed, in/sec(cm/sec)
V10A	1850(1010)	12	5.9(15.0)
V10B	1850(1010)	16	4.9(12.4)
V10C	1850(1010)	22	3.7 (9.4)
V10D	1950(1065)	12	7.6(19.3)
V10E	1950(1065)	16	6.9(17.5)
V10F	1950(1065)	22	5.0(12.7)
V10G	2050(1120)	12	8.2(20.8)
V10H	2050(1120)	16	7.5(19.1)
V10I	2050(1120)	22	5.4(13.7)
V21A	1750 (955)	26	2.0 (5.1)
V21B	1950(1065)	30	4.7(11.9)
V21C	2150(1175)	36	NR*
V21D	2150(1175)	26	NR
V21E	2150(1175)	18	NR
V21F	1900(1040)	18	4.4(11.2)
V21G	2050(1120)	30	4.2(10.7)
V21H	2150(1175)	50	3.2 (8.1)
V21I	2200(1205)	50	7.4(18.8)
V22A	1900(1040)	18	3.8 (9.7)
V22B	2150(1175)	50	5.9(15.0)
V22C	2150(1175)	36	7.1(18.0)
V22D	2150(1175)	18	8.3(18.0)
V22E	2000(1095)	50	8.3(21.1)
V22F	2200(1205)	18	9.4(23.9)
V22G	2050(1120)	36	4.9(12.4)
V22H	2200(1205)	50	5.8(14.7)

*No Record

+100% Throttle

TABLE VI

EXTRUSION CONDITIONS FOR ALLOYS 5, 6, 7 AND 8 EXTRUSIONS

Alloy No.	Billet No.	Temp. °F(°C)	Ratio	% Throttle	Speed in/sec (cm/sec)
5	V31-A	2150(1175)	55	100	8.9(22.6)
5	V31-B	2150(1175)	22	100	12.5(31.8)
5	V31-C	2050(1120)	55	100	4.4(11.2)
5	V31-D	2050(1120)	22	100	12.1(30.7)
5	V31-E	2150(1175)	20	30	3.8 (9.7)
5	V31-F	2050(1120)	20	30	3.2 (8.1)
6	V33-A	2150(1175)	55	100	6.9(17.5)
6	V33-B	2150(1175)	22	100	14.9(37.8)
6	V33-C	2050(1120)	55	100	8.1(20.6)
6	V33-D	2050(1120)	21	100	12.9(32.8)
6	V33-E	2150(1175)	20	30	3.6 (9.1)
6	V33-F	2150(1175)	20	30	3.8 (9.7)
7	V35-A	2150(1175)	55	100	5.9(15.0)
7	V35-B	2150(1175)	20	100	14.5(36.8)
7	V35-C	2050(1120)	55	100	3.2 (8.1)
7	V35-D	2050(1120)	20	100	10.5(26.7)
7	V35-E	2150(1175)	20	30	3.8 (9.7)
7	V35-F	2050(1120)	20	30	3.6 (9.1)
8	V37-A	2150(1175)	55	30	2.0 (5.1)
8	V37-B	2150(1175)	20	30	4.0(10.2)
8	V37-C	2050(1120)	55	100	3.0 (7.6)
8	V37-D	2050(1120)	20	100	12.1(30.7)
8	V37-E	2150(1175)	30	100	11.7(29.7)
8	V37-F	2050(1120)	20	30	3.2 (8.1)

TABLE VII

RECRYSTALLIZATION RESPONSE OF ALLOY 1 AND ALLOY 2 EXTRUDED BARS

Bar No.	Conv. Anneal[1] Temp., °F(°C)	Structure	GAR	Zone Anneal Temp., °F(°C) /Rate iph(cmph)	Structure	GAR
V10A[2]	2350(1290)	Partial Rx	--			
V10B	"	No Rx	--			
V10C	"	M.Eq.	--			
V10D	"	No Rx	--			
V10E	"	M.Eq.	--			
V10F	"	M.Eq.	--			
V10G	"	Partial Rx	--			
V10H	"	Partial Rx	--			
V10I	"	No Rx	--			
V21A[3]	2350(1290)	M.Eq.	~1	-- -- -- --	-	-
V21B	"	C.Eq.	2.7	2410(1321)/5.2(13.2)	C.El-M.Eq.	2.6
V21C	"	C.El-C.Eq.	4.5	2420(1327)/5.2(13.2)	C.El-C.Eq.	4.6
V21D	"	C.Eq.	2.0	2375(1302)/5.3(13.5)	C.Eq.	1.9
V21E	"	C.El-M.Eq.	3.4	2415(1324)/5.2(15.7)	C.El-M.Eq.	4.0
V21F	2400(1315)	C.El-M.Eq.	2.6	2410(1315)/5.3(13.5)	M.Eq.	2.0
V21G	"	C.Eq.	3.8	2375(1302)/5.3(13.5)	C.El.	>10
V21H	"	C.El.	6.1	2375(1302)/5.3(13.5)	C.El.	8.4
V21I	"	C.El.	7.3	2385(1307)/5.3(13.5)	C.El.	8.0
V22A[4]	2400(1315)	M.Eq.	~1	-- -- -- --	-	-
V22B	"	C.El-C.Eq.	4.5	2355(1291)/5.3(13.5)	C.El.	6.5
V22C	"	C.El-M.Eq.	3.2	2360(1293)/5.3(13.5)	C.El-M.Eq.	3.0
V22D	"	C.El-M.Eq.	3.8	2370(1297)/5.3(13.5)	C.El-M.Eq.	4.0
V22E	"	No Rx	-	-- -- -- --	-	-
V22F	"	C.El-M.Eq.	2.3	-- -- -- --	-	-
V22G	2350(1290)	C.El-C.Eq.	3.5	-- -- -- --	-	-
V22H	"	C.El-M.Eq.	2.0	-- -- -- --	-	-

* No Record
[1] Temperature of Best Structure.
[2] Batch V10 = Alloy 1 Composition.
[3] Batch V21 = Alloy 2 Composition.
[4] Batch V22 = Alloy 1 Composition.

Structural Definitions:

Rx = Recrystallization
M.Eq. = Medium Equiaxed
C.Eq. = Coarse Equiaxed
C.El. = Coarse Elongated

TABLE VIII

VOLUME FRACTIONS OF γ' IN ALLOYS 1 AND 2

Alloy	Sample No.	Heat Treatment, °F(°C)	% γ'
1	V22B-36	2350(1290)/1/2 hr/FC	97
1	V22B-35	2350(1290)/1/2 hr/AC	95
1	V22B-34	2350(1290)/1/2 hr/WQ	0
1	V22B-33	2100(1150)/1/2 hr/WQ	80
1	V22B-32	2000(1095)/1/2 hr/WQ	90
2	V21C-43	2350(1290)/1/2 hr/FC	90
2	V21C-42	2350(1290)/1/2 hr/AC	85
2	V21C-41	2350(1290)/1/2 hr/WQ	0
2	V21C-40	2100(1150)/1/2 hr/WQ	50
2	V21C-39	2000(1095)/1/2 hr/WQ	60

FC = Furnace Cool

AC = Air Cool

WQ = Water Quench

TABLE IX

2000°F(1095°C) STRESS RUPTURE RESULTS FOR ALLOY 1 BARS

Bar No.	Heat Treatment, °F(°C)	GAR	Stress, ksi (MPa)	Life, hrs	% El	% RA
V22A	2400(1315)/1/2 hr/AC	1	14 (96.5)	0.1	nil	nil
V22A	2400(1315)/1/2 hr/AC	1	10 (69.0)	6.9	1.3	nil
V22B	2350(1290)/1/2 hr/AC	4.5	12 (82.7)	24.0	STEP LOAD	
V22B	2350(1290)/1/2 hr/AC	4.5	14 (96.5)	12.5	1.3	1.5
V22B	2400(1315)/1/2 hr/AC	4.5	14 (96.5)	1.3	nil	nil
V22B	2400(1315)/1/2 hr/AC	4.5	10 (69.0)	3.3	2.5	3.0
V22B	*ZA2355°F(1291°C)/5.3 iph(13.5 cmph)	6.5	14 (96.5)	3.5	1.3	2.9
V22C	2400(1315)/1/2 hr/AC	3.2	14 (96.5)	3.0	2.5	1.5
V22C	2400(1315)/1/2 hr/AC	3.2	10 (69.0)	10.0	1.3	1.5
V22C	*ZA2360°F(1293°C)/5.3 iph(13.5 cmph)	3.0	14 (96.5)	0.6	2.5	2.9
V22D	2350(1290)/1/2 hr/AC	3.8	12 (82.7)	23.8	STEP LOAD	
V22D	2350(1290)/1/2 hr/AC	3.8	14 (96.5)	48.0	STEP LOAD	
V22D	2350(1290)/1/2 hr/AC	3.8	16(110.0)	2.4	1.3	1.5
V22D	2400(1315)/1/2 hr/AC	3.8	14 (96.5)	24.0	STEP LOAD	
V22D	2400(1315)/1/2 hr/AC	3.8	16(110.0)	1.0	1.3	1.4
V22D	2400(1315)/1/2 hr/AC	3.8	10 (69.0)	528.0+	TEST TERMINATED	
V22D	*ZA2370°F(1297°C)/5.3 iph(13.5 cmph)	4.0	14 (96.5)	24.0	STEP LOAD	
			16(110.0)	1.7	1.3	2.9

* Zone Anneal

+ Specimen not broken

TABLE X

2000°F(1095°C) STRESS RUPTURE RESULTS FOR CONVENTIONAL ANNEALED* ALLOY 2 BARS

Bar No.	GAR	Stress, ksi (MPa)	Life, hrs	% El	% RA
V21A	1	14(96.5)	3.4	1.3	2.9
V21B	2.7	14(96.5)	0.8	2.5	3.0
		12(82.7)	2.9	1.3	2.9
		10(69.0)	0.6	1.3	1.4
V21C	4.5	14(96.5)	0.0	1.3	nil
		12(82.7)	1.1	2.5	4.3
		10(69.0)	0.2	1.3	1.4
V21D	2.0	14(96.5)	0.1	1.3	nil
		12(82.7)	1.1	1.3	2.9
		10(69.0)	0.0	2.5	1.5
V21E	3.4	14(96.5)	15.9	1.3	nil
		12(82.7)	24.0	STEP LOAD	
		14(96.5)	24.0	STEP LOAD	
		16(110)	6.9	2.5	2.9
		10(69.0)	297.0	1.3	1.4
V21F	2.6	14(96.5)	3.2	1.3	1.4
		12(82.7)	24.0	STEP LOAD	
		14(96.5)	12.0	nil	nil
		10(69.0)	41.2	5.0	3.0
V21G	3.8	14(96.5)	6.1	1.3	nil
		10(69.0)	158.2	2.5	nil
V21H	6.1	14(96.5)	6.0	1.3	3.0
		10(69.0)	114.2	nil	nil
+V21I	7.3	14(96.5)	0.3	nil	nil
		12(82.7)	24.0	STEP LOAD	
		14(96.5)	0.1	2.5	nil

* 2350°F(1290°C)/1/2 hr/AC

\+ 2400°F(1315°C)/1/2 hr/AC (Probable Incipient melting)

TABLE XI

2000°F(1095°C) STRESS RUPTURE TEST RESULTS FOR ZONE ANNEALED* ALLOY 2 BARS

Bar No.	GAR	Stress, ksi (MPa)	Life, hrs	% El	% RA
V21B	2.6	14 (96.5)	3.0	nil	nil
V21C	4.6	14 (96.5)	0.4	2.5	4.3
V21D	1.9	14 (96.5)	0.1	1.3	2.9
V21E	4.0	14 (96.5)	25.4	1.3	2.9
V21F	2.0	14 (96.5)	1.4	1.3	2.9
V21G	>10	14 (96.5)	24.0	STEP	LOAD
"	>10	16(110)	24.0	"	"
"	>10	18(124)	1.6	1.3	2.9
V21G	>10	16(110)	61.0	2.5	5.8
+V21G	>10	15(103)	44.7	2.5	8.5
V21G	>10	14 (96.5)	769.4	2.5	4.3
V21H	8.4	14 (96.5)	24.0	STEP	LOAD
"	8.4	16(110)	4.8	7.5	11.1
V21H	8.4	14 (96.5)	8.6	1.3	1.9
V21I	8.0	14 (96.5)	8.0	2.5	2.9
V21I	8.0	14 (96.5)	24.0	STEP	LOAD
"	8.0	16(110)	19.1	3.8	8.6
V21I	8.0	14 (96.5)	97.4	1.3	7.2

* Zone annealed at approximately 2395°F(1312°C)/5.3 iph(13.5 cmph)

+ Creep test. See Figure 30.

TABLE XII

ALLOY 2 ZONE ANNEALED* STRESS RUPTURE PROPERTIES

Bar No.	Temp., °F(°C)	Stress, ksi (MPa)	Life, hrs	% El	% RA
V21I	1400 (760)	85(586)	20.1	2.5	4.3
V21I	1400 (760)	70(482)	156.7	3.8	7.2
V21G	2000(1095)	18(124)	1.6	1.3	2.9
V21G+	2000(1095)	16(110)	61.0	2.5	5.8
V21G+	2000(1095)	15(103)	44.7	2.5	8.5
V21G	2000(1095)	14 (96.5)	769.4	2.5	4.3
V21G	2100(1150)	12 (82.7)	53.4	5.0	8.5
V21G	2100(1150)	10 (69.0)	1005.7	3.8	8.7

* Tested as annealed

+ Tested ZA + 2350°F(1290°C)/1/2 hr/AC

TABLE XIII

ALLOY 2 1400°F(760°C)/70 ksi(482 MPa) CREEP RUPTURE PROPERTIES

Bar No.	Heat Treat	Rupture Life hrs	Prior Creep % el	Rupture Ductility % El	Rupture Ductility % RA	Creep Rate hr
V21G-32	ZA + D	52.4	1.2	2.5	5.7	19.0×10^{-5}
V21G-30	ZA + A	114.0	0.7	1.3	2.9	5.5×10^{-5}
V21G-22	ZA + B	108.8	1.1	2.5	4.3	4.6×10^{-5}
V21G-25	ZA + C	163.5	2.5	3.8	7.2	5.3×10^{-5}

ZA: Zone Annealed @ ∿ 2395°F(1312°C)/5.3 iph(13.5 cmph)

A: 2350°F(1290°C)/1/2 hr/oil quench

B: 2350°F(1290°C)/1/2 hr/air cool + 2190°F(1200°C)/1/2 hr/oil quench

C: 2350°F(1290°C)/1/2 hr/air cool + 2085°F(1140°C)/1/2 hr/oil quench

D: 2350°F(1920°C)/1/2 hr/air cool

TABLE XIV

1400°F(760°C) STRESS RUPTURE RESULTS FOR ALLOY 7 AND 8 BARS

Alloy No.	Bar No.*	GAR	Stress, ksi (MPa)	Life, hrs	% El	% RA
7	V35-D	>10:1	70(482)	24.0	STEP	LOAD
			75(517)	24.0	"	"
			80(552)	24.0	"	"
			85(586)	26.9	3.8	6.1
7	V35-D	>10:1	75(517)	190.0	2.5	2.7
8	V37-F	5:1	70(482)	24.0	STEP	LOAD
			75(517)	24.0	"	"
			80(552)	7.5	2.5	2.9
8	V37-F	5:1	75(517)	90.6	1.3	1.4

* Bars Zone Annealed at 2275°F(1247°C)/5.3 iph(13.5 cmph)

TABLE XV

2000°F(1095°C) AND 2100°F(1150°C) STRESS RUPTURE RESULTS FOR ALLOYS 7 AND 8 BARS

Alloy No.	Bar No.*	GAR	Temp., °F(°C)	Stress, ksi (MPa)	Life, hrs	% El	% RA
7	V35-D	>10:1	2000(1095)	14 (96.5)	24.0	STEP	LOAD
"	"	"	"	16(110)	24.0	"	"
"	"	"	"	18(124)	24.0	"	"
"	"	"	"	20(138)	24.0	"	"
"	"	"	"	22(152)	6.1	3.8	2.9
7	V35-D	>10:1	2000(1095)	18(124)	204.1	1.3	1.5
7	V35-D	>10:1	2100(1150)	14 (96.5)	90.3	3.8	4.3
7	V35-D	>10:1	2100(1150)	16(110)	13.6	2.5	2.9
8	V37-F	>10:1	2000(1095)	14 (96.5)	24.2	STEP	LOAD
"	"	"	"	16(110)	24.0	"	"
"	"	"	"	18(124)	24.0	"	"
"	"	"	"	20(138)	20.2	2.5	3.0
8	V37-F	>10:1	2000(1095)	18(124)	612.5	1.3	1.5
8	V37-F	>10:1	2100(1150)	14 (96.5)	222.3	1.3	2.9
8	V37-F	>10:1	2100(1150)	16(110)	25.2	2.5	2.9

* Bars Zone Annealed 2275°F(1247°C)/5.3 iph(13.5 cmph)

TABLE XVI

DENSITY OF ALLOYS 2, 7 AND 8

Alloy No.	Composition, Wt.%					ρ, lbs/in^3(gm/cm^3)
	Ni	Cr	Al	W	Y_2O_3	
2	81.1	9.9	9.0	-	1.1	.275(7.60)
7	78.1	9.7	8.8	3.4	1.1	.277(7.66)
8	75.3	9.5	8.6	6.7	1.1	.295(8.17)

TABLE XVII

ALLOY 2 TENSILE PROPERTIES

Bar No.	Heat Treat	.2% YS, ksi (MPa)	UTS, ksi (MPa)	% El	% RA	Modulus x 10^6 psi (10^9 Pa)
		Room Temperature Results				
V21H	ZA	106.5(734)	135.8 (936)	3.5	10.0	27.4(189)
V21G	ZA + A	132.1(910)	187.9(1295)	7.0	8.5	19.8(136)
V21G	ZA + B	122.8(846)	175.5(1209)	7.0	9.0	21.9(151)
V21G	ZA + C	121.1(834)	190.4(1312)	7.0	10.5	18.2(125)
V21G	ZA + D+	119.2(821)	158.9(1095)	5.5	5.5	23.8(164)
Cast Mar M-200	-	120 (827)	135 (930)	7.0	-	31.6(218)
		1400°F(760°C) Results				
V21H	ZA	95.5(658)	104.3 (719)	2.0	3.5	10.9 (75.1)
V21G	ZA + A	133.2(918)	142.6 (983)	3.5	5.5	8.2 (56.5)
V21G	ZA + B	108.7(749)	123.3 (850)	2.0	5.0	9.0 (62.0)
V21G	ZA + C	118.1(814)	134.7 (928)	2.0	7.5	10.4 (71.7)
V21G	ZA + D+	108.2(745)	115.4 (795)	3.5	6.5	9.6 (66.1)
Cast Mar M-200	-	122 (841)	135 (930)	3.4	-	25.8(178.0)

ZA: Zone annealed @ ~ 2395°F(1300°C)/5.3 in/hr(13.5 cm/hr)

A: 2350°F(1295)C)/1/2 hr/oil quench

B: 2350°F(1290°C)/1/2 hr/air cool + 2190°F(1200°C)/1/2 hr/oil quench

C: 2350°F(1290°C)/1/2 hr/air cool + 2085°F(1140°C)/1/2 hr/oil quench

D: 2350°F(1285°C)/1/2 hr/water quench

\+ Quench cracks observed

TABLE XVIII

BURNER RIG SULFIDATION TEST RESULTS*

Alloy	Test Duration hrs	ΔW, undesc. -10^{-3} lb/in^2 (-mg/cm^2)	ΔW, desc. -10^{-3} lb/in^2 (-mg/cm^2)	Metal Loss 10^{-4} in(μm)	Maximum Attack 10^{-4} in(μm)
V21I	168	3.24(228)	3.99(281)	563(1430)	586(1488)
V21I	168	3.72(262)	4.25(299)	569(1443)	630(1600)
V22D	168	1.68(118)	2.39(168)	333 (846)	407(1034)
V22D	168	0.55 (39)	1.33 (94)	223 (566)	309 (785)
IN-100	72	DESTROYED			
Alloy 713C	120	DESTROYED			
UDIMET 500	168	0.014(-1.0)	0.29(20.6)	20 (51)	89 (226)
IN-738	168	0.011(-0.8)	0.12 (8.3)	11 (28)	33 (84)
MA755E	168	0.0(-0.0)	0.16(11.2)	15 (38)	73 (185)

* CONDITIONS: 1700°F(927°C)(58 minutes) followed by 2 minute air blast. 30:1 Air + 5ppm seawater (ASTM Spec. D1141-52) to fuel (.3% sulfur JP-5) ratio.

V21 Alloy 2 (Ni-9.9 wt.% Cr-9.0 wt.% Al-1.1 wt.% Y_2O_3)

V22 Alloy 1 (Ni-10.1 wt.% Cr-10.4 wt.% Al-1.1 wt.% Y_2O_3)

TABLE XIX

2012°F(1100°C) CYCLIC OXIDATION TEST RESULTS* FOR ALLOY 2

Alloy	Test Duration hrs	ΔW, undesc. -10^{-3} lb/in^2 (-mg/cm^2)	ΔW, desc. -10^{-3} lb/in^2 (-mg/cm^2)
V21G-1	504	0.016 (1.15)	0.035 (2.47)
V21G-2	504	0.014 (1.00)	0.033 (2.30)
IN-100	504	0.042 (2.99)	0.10 (7.27)
Alloy 713C	504	0.28 (19.42)	0.30 (21.05)
IN-738	504	0.87 (61.46)	1.02 (71.91)
MA755E	504	0.21 (14.51)	0.26 (18.03)

* CONDITIONS: Air-5% H_2O flowing at 15 in^3/min(250 cc/min). Samples cycled to room temperature every 24 hours.

TABLE XX

1000 HOUR SPECIFIC RUPTURE STRENGTH-TEMPERATURE DATA FOR FIGURE 33

Alloy	Density ρ, lbs/in^3 (gm/cm^3)	Temp., °F (°C)	Stress, σ ksi (MPa)	σ/ρ in x 10^3 (cm x 10^3)
*DS Mar M-200 + Hf	.312 (8.63)	1400 (760)	92 (634)	295 (749)
		1600 (870)	48 (749)	154 (391)
		1800 (980)	16.2 (112)	52 (132)
*DS Eutectic $\gamma/\gamma'-\alpha$	.307 (8.50)	1400 (760)	102 (703)	322 (843)
		1600 (870)	57 (393)	186 (472)
		1800 (980)	25.5 (176)	83 (211)
		2000 (1095)	11.5 (79)	37 (94)
		2100 (1150)	6.5 (45)	21.2 (54)
Alloy 8	.295 (8.15)	1400 (760)	71 (490)	241 (612)
		2000 (1095)	17.9 (123)	61 (155)
		2100 (1150)	12.9 (89)	44 (112)

* From Reference 9

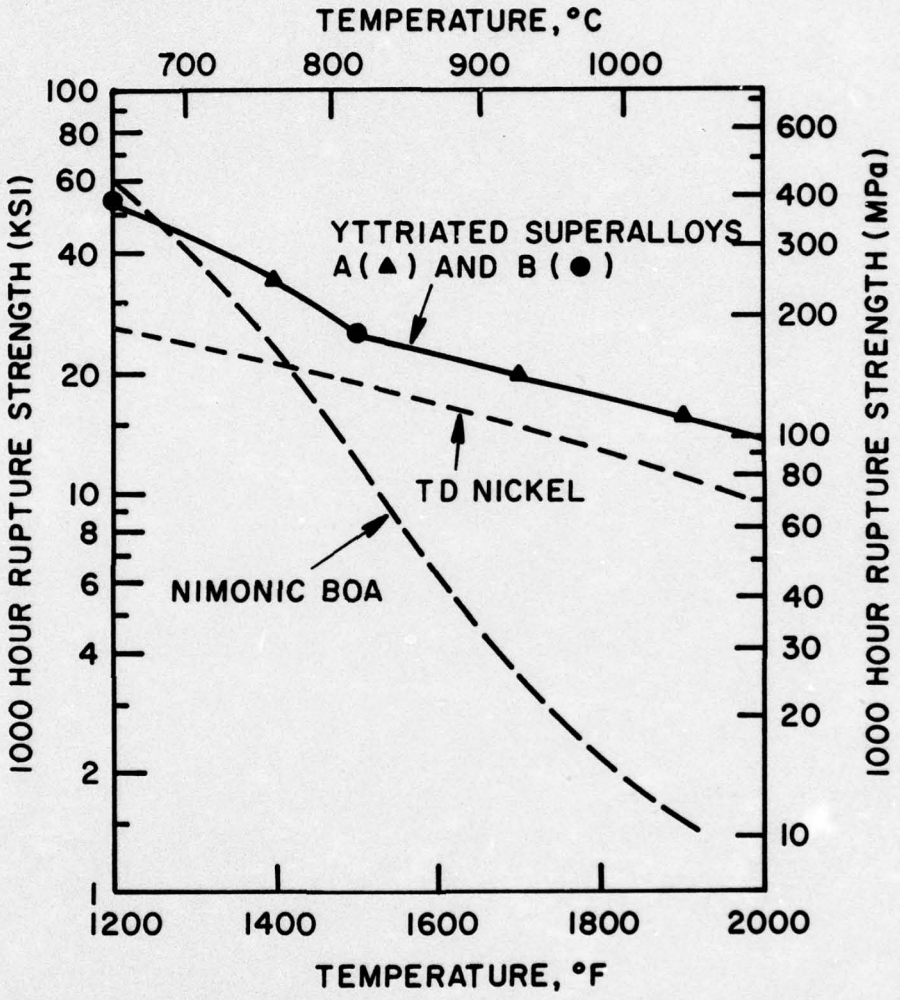

FIGURE 1 - STRESS FOR 1000 HOUR LIFE IN YTTRIATED SUPERALLOYS AS A FUNCTION OF TEMPERATURE. (FROM REFERENCE 4)

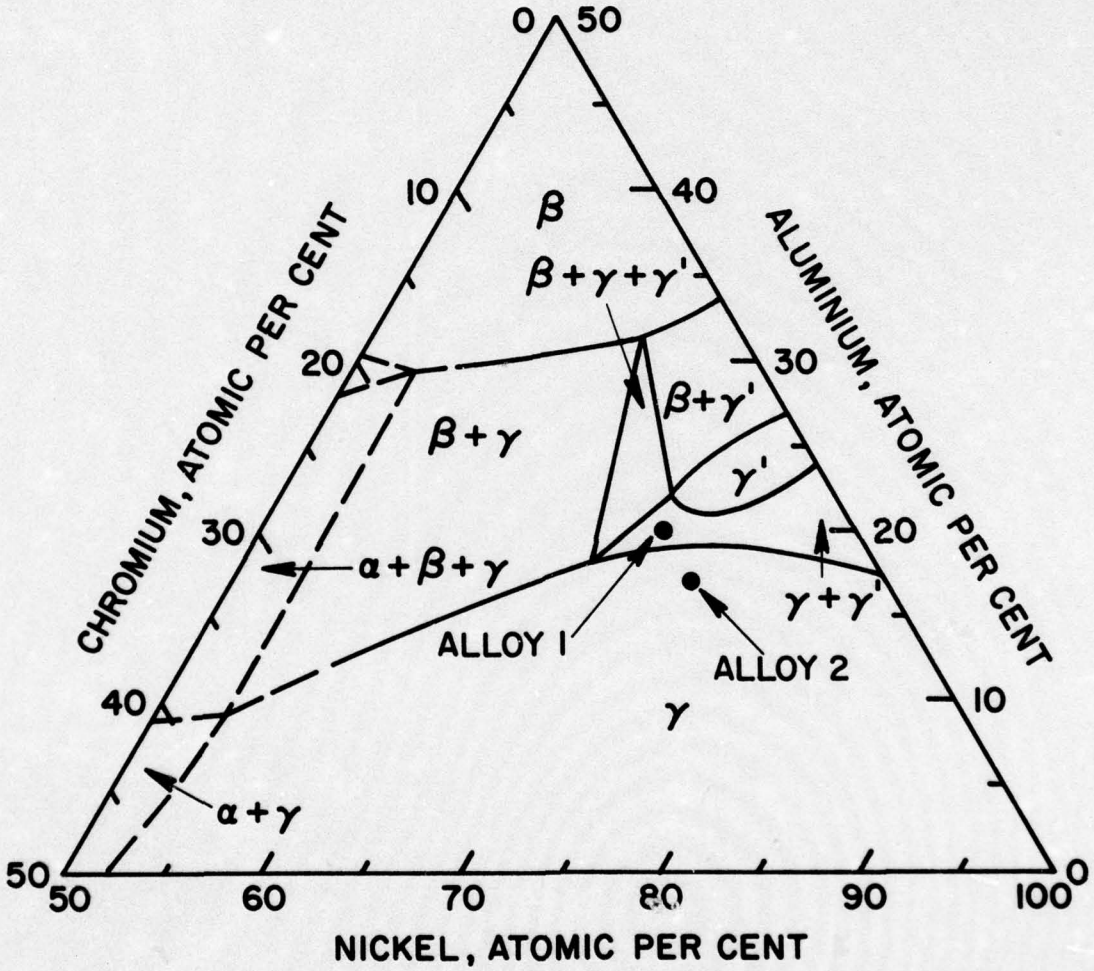

FIGURE 2 - THE Ni-Cr-Al PHASE DIAGRAM: ISOTHERMAL SECTION FOR 1150°C (AFTER TAYLOR AND FLOYD, JOURNAL INST. OF METALS, 1952-1953, VOLUME 81, P. 451.).

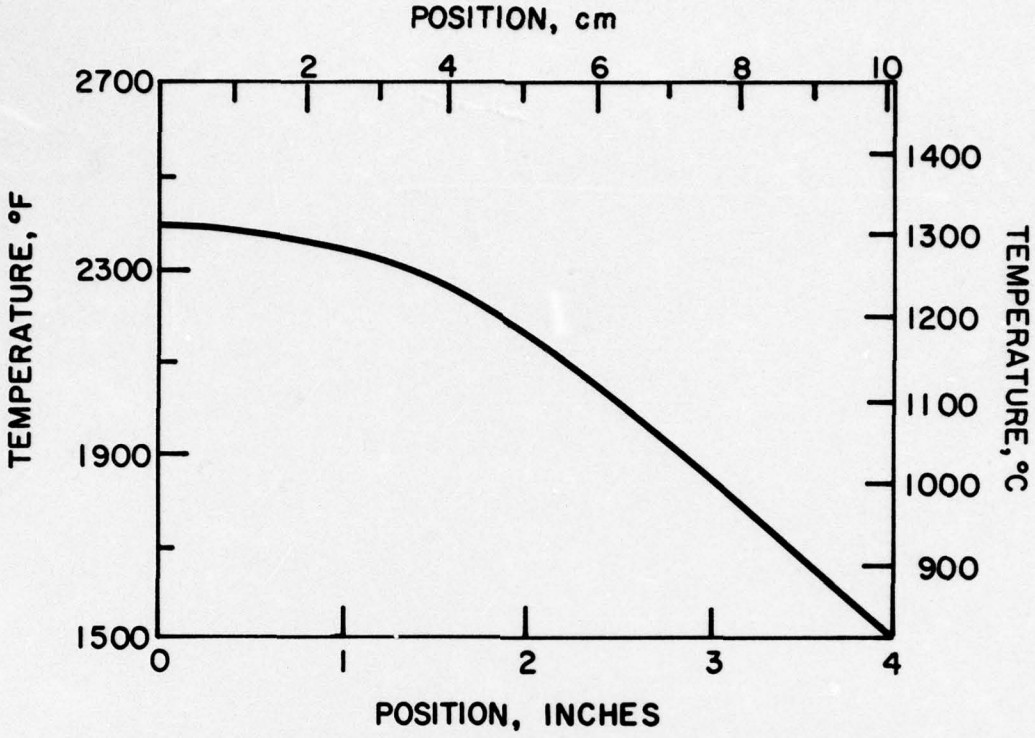

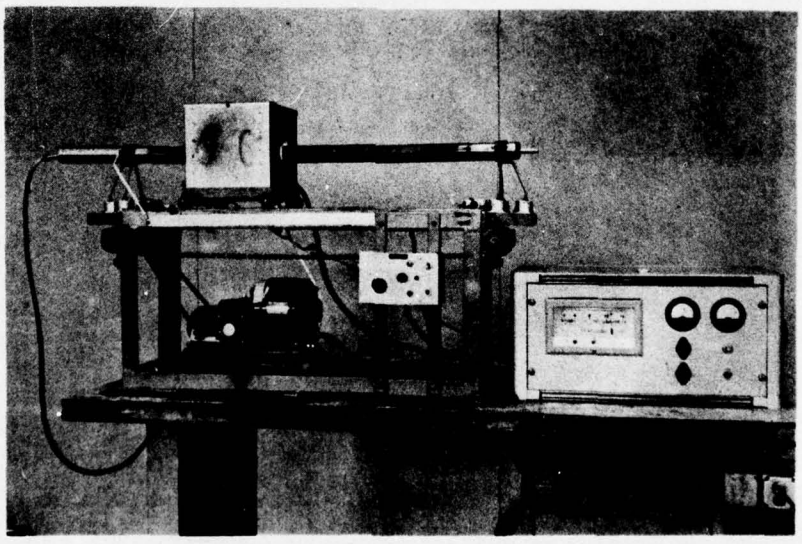

Figure 3 - Temperature Profile and Furnace Used for Gradient and Zone Annealing

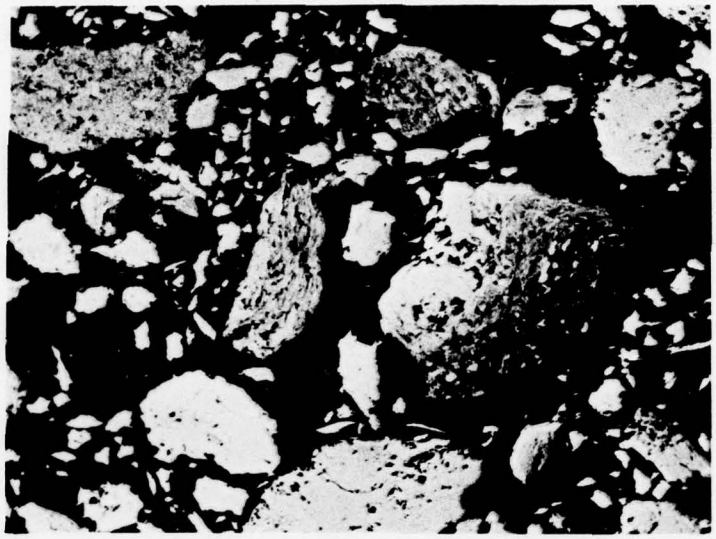

P.N. 1-48329 50X

(a)

P.N. 1-48330 250X

(b)

Figure 4 - Micrographs of Attrited Powder of Alloy 1, Batch V2

Etchant: 50:50 Cyanide Persulfate

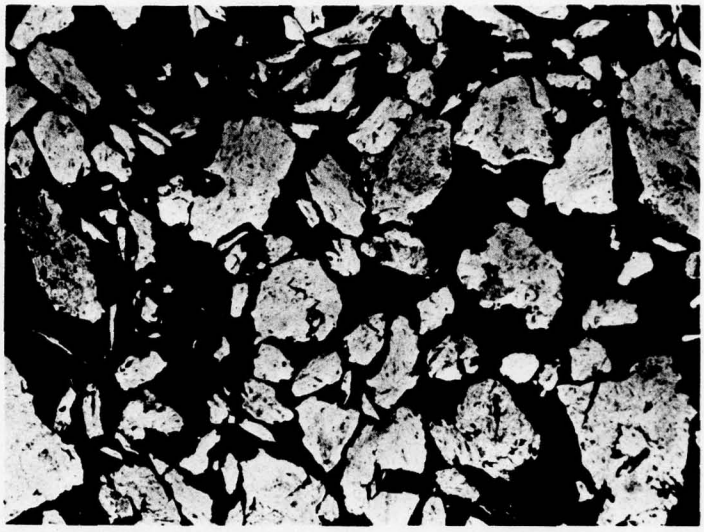

P.N. 1-49171 100X

(a)

P.N. 1-49174 100X

(b)

Figure 5 - Micrographs of Attrited Powder of Alloy 1, Batch V4

Etchant: 50:50 Cyanide Persulfate

P.N. 1-49167 100X

(a)

P.N. 1-49170 100X

(b)

Figure 6 - Micrographs of Attrited Powder of Alloy 2, Batch V12

Etchant: 50:50 Cyanide Persulfate

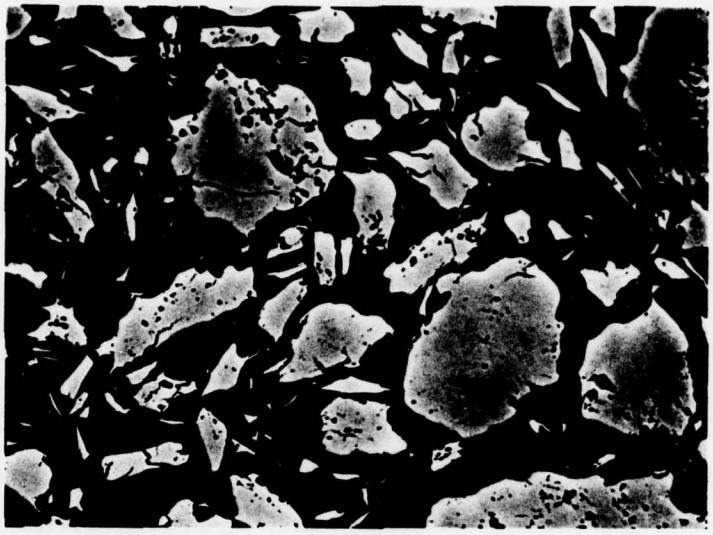

P.N. 1-49611 50X

(a)

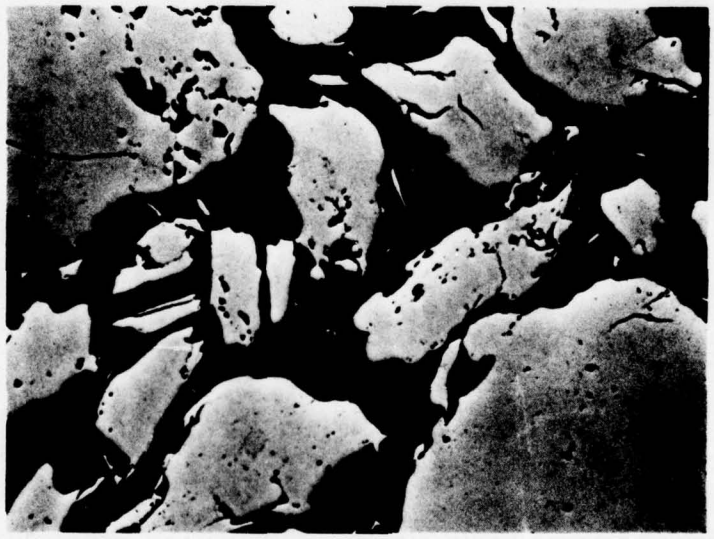

P.N. 1-49612 250X

(b)

Figure 7 - Micrographs of Attrited Powder of Alloy 1, Batch V17

Etchant: 50:50 Cyanide Persulfate

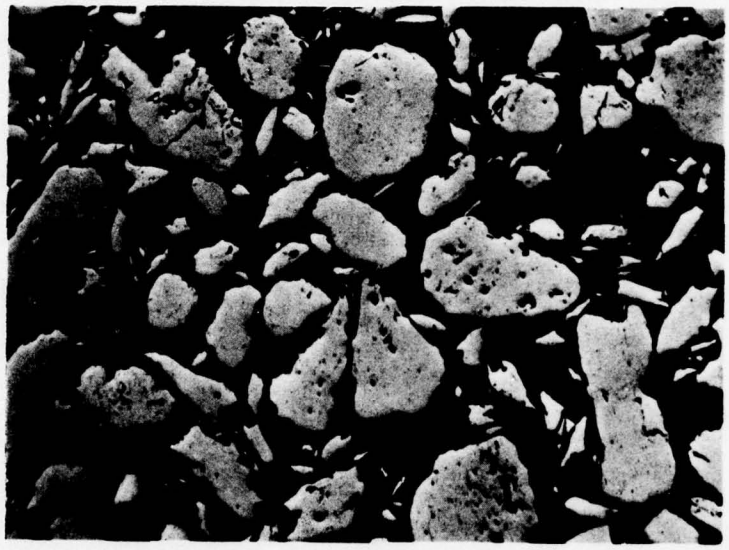

P.N. 1-54689 50X

(a)

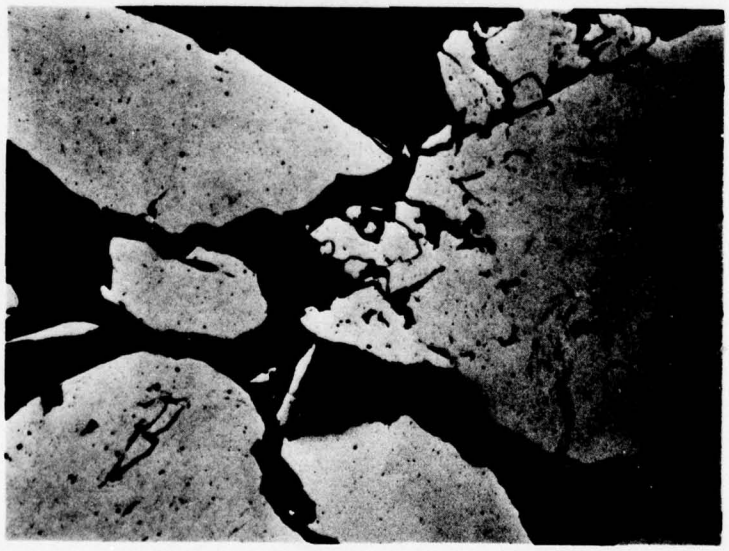

P.N. 1-54690 250X

(b)

Figure 8 - Micrographs of Attrited Powder of Alloy 5, Batch V31

Etchant: 50:50 Cyanide Persulfate

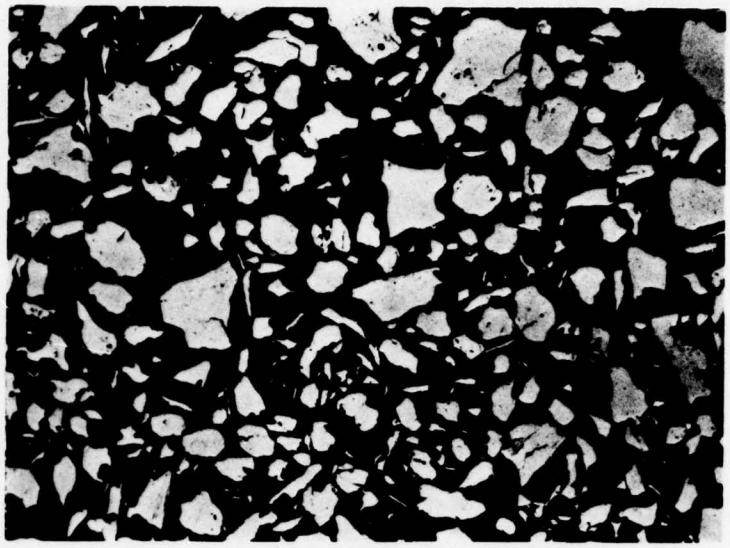

P.N. 1-54997 50X

(a)

P.N. 1-54998 250X

(b)

Figure 9 - Micrographs of Attrited Powder of Alloy 6, Batch V34

Etchant: 50:50 Cyanide Persulfate

P.N. 1-55109 50X

(a)

P.N. 1-55110 250X

(b)

Figure 10 - Micrographs of Attrited Powder of Alloy 7, Batch V36

Etchant: 50:50 Cyanide Persulfate

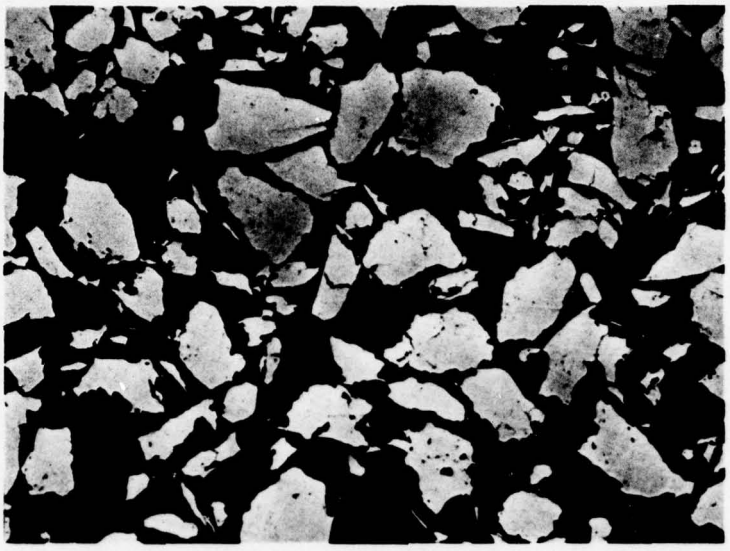

P.N. 1-55442 50X

(a)

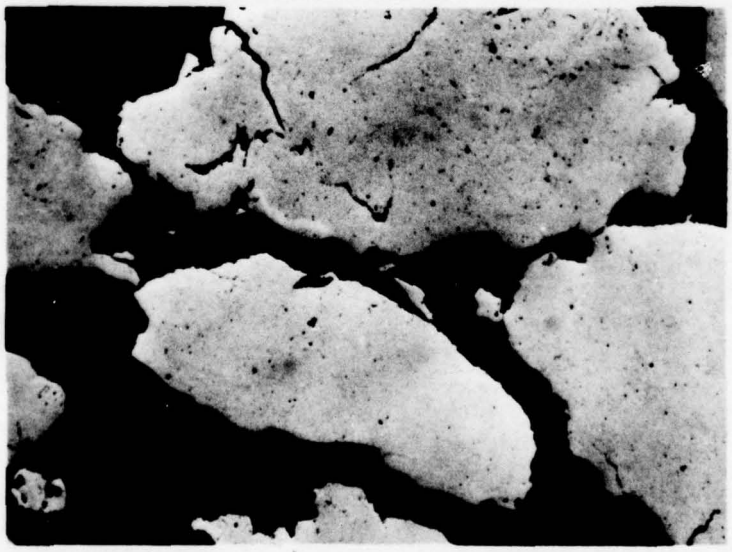

P.N. 1-55443 250X

(b)

Figure 11 - Micrographs of Attrited Powder of Alloy 8, Batch V37

Etchant: 50:50 Cyanide Persulfate

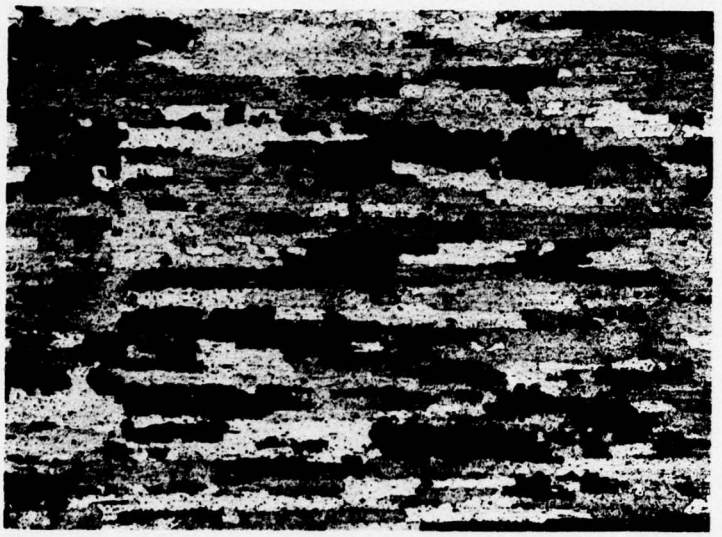

P.N. 1-50127 50X

(a) Bar V22A Extruded 1900°F (1040°C)/ 18:1/3.8 in/sec (9.7 cm/sec). Annealed 2400°F (1315°C)/1/2 hr/AC (M.EQ.)

P.N. 1-50140 50X

(b) Bar V22B Extruded 2150°F (1175°C)/ 50:1/5.9 in/sec (15.0 cm/sec). Annealed 2400°F (1315°C)/1/2 hr/AC (C.El-C.EQ.)

Figure 12 - Microstructures of Typical Alloy 1, V22 Extrusions

Etchant: 45:45:10 $HCl:H_2O:H_2O_2$

P.N. 1-50130 50X

(c) Bar V22C Extruded 2150°F (1175°C)/ 36:1/7.1 in/sec (18.0 cm/sec). Annealed 2400°F (1315°C)/1/2 hr/AC (C.El-M.EQ.)

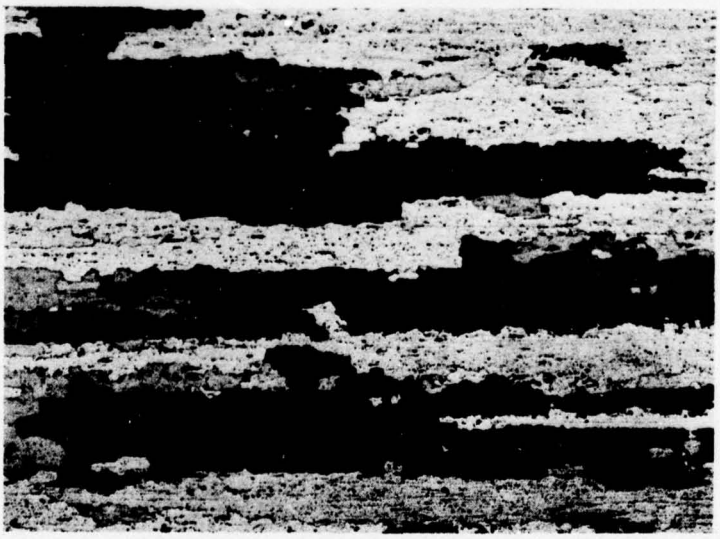

P.N. 1-50131 50X

(d) Bar V22D Extruded 2150°F (1175°C)/ 18:1/8.3 in/sec (21.1 cm/sec). Annealed 2400°F (1315°C)/1/2 hr/AC (C.El-M.EQ.)

Figure 12 - Continued

P.N. 1-50922 50X

(e) Bar V22F Extruded 2200°F (1205°C)/ 18:1/9.4 in/sec (23.9 cm/sec). Annealed 2400°F (1315°C)/1/2 hr/AC (C.El-M.EQ.)

P.N. 1-51808 50X

(f) Bar V22G Extruded 2050°F (1120°C)/ 30:1/4.9 in/sec (12.4 cm/sec). Annealed 2350°F (1290°C)/1/2 hr/AC (C.El-C.EQ.)

Figure 12 - Continued

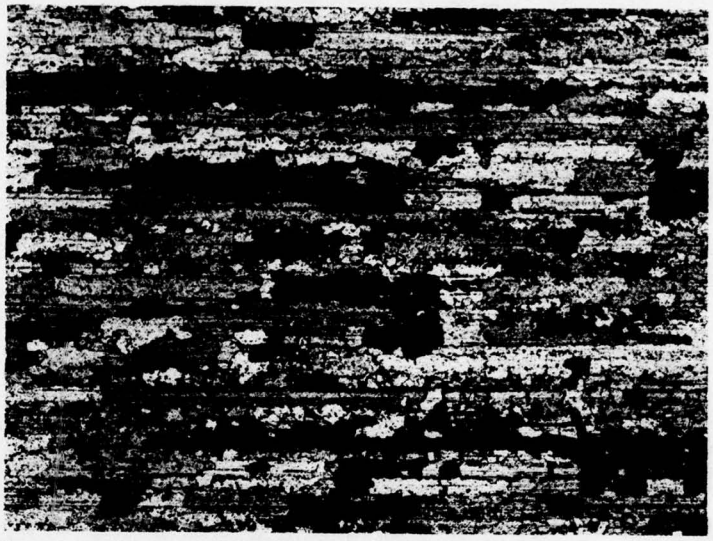

P.N. 1-51810 50X

(g) Bar V22H Extruded 2200°F (1205°C)/ 50:1/5.8 in/sec (14.7 cm/sec). Annealed 2350°F (1290°C)/1/2 hr/AC (C.El-M.EQ.)

Figure 12 - Continued

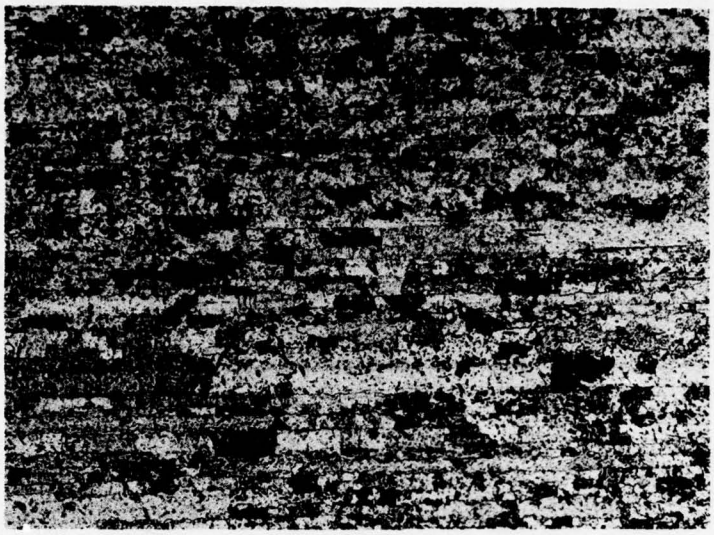

P.N. 1-49758 100X

(a) Bar V21A Extruded 1750°F (955°C)/ 26:1/2.0 in/sec (5.1 cm/sec). Annealed 2350°F (1290°C)/1/2 hr/AC (M.EQ.)

P.N. 1-49759 50X

(b) Bar V21B Extruded 1950°F (1065°C)/ 30:1/4.7 in/sec (11.9 cm/sec). Annealed 2350°F (1290°C)/1/2 hr/AC (C.EQ.)

Figure 13 - Microstructures of Typical Alloy 2, V21 Extrusions.

Etchant: 45:45:10 $HCl:H_2O:H_2O_2$

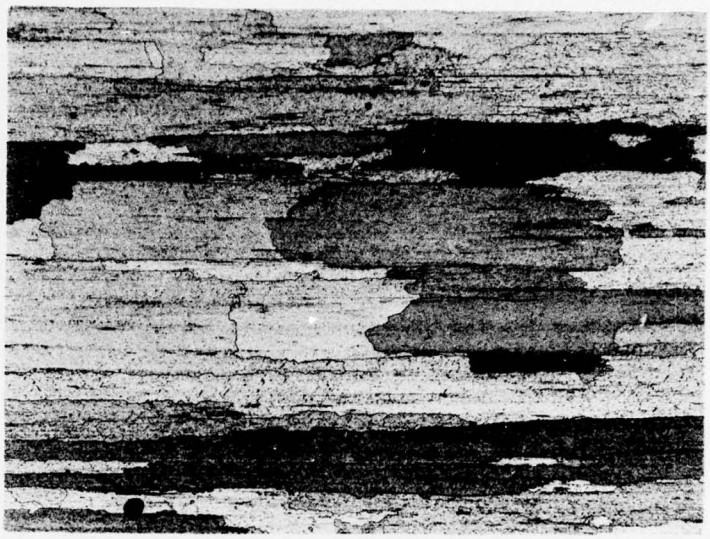

P.N. 1-49761 50X

(c) Bar V21C Extruded 2150°F (1175°C)/ 36:1/NR. Annealed 2350°F (1290°C)/ 1/2 hr/AC (C.El-C.EQ.)

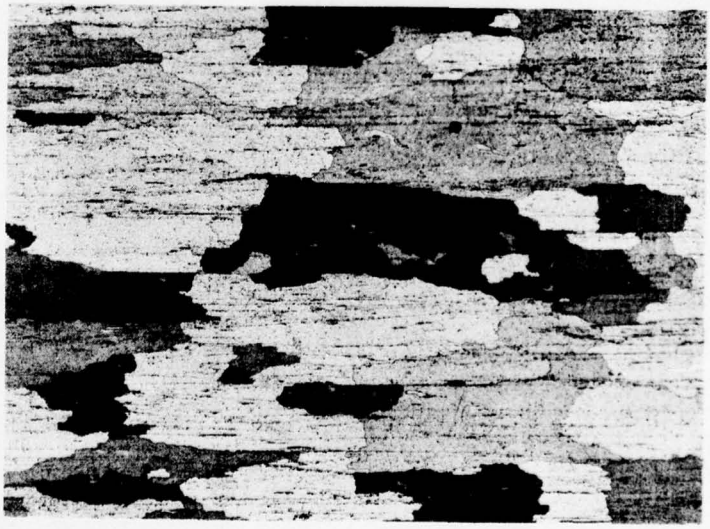

P.N. 1-49764 50X

(d) Bar V21D Extruded 2150°F (1175°C)/ 26:1/NR. Annealed 2350°F (1290°C)/ 1/2 hr/AC (C.EQ.)

Figure 13 - Continued

P.N. 1-49765 50X

(e) Bar V21E Extruded 2150°F (1175°C)/ 18:1/NR. Annealed 2350°F (1290°C)/ 1/2 hr/AC (C.E1-M.EQ.)

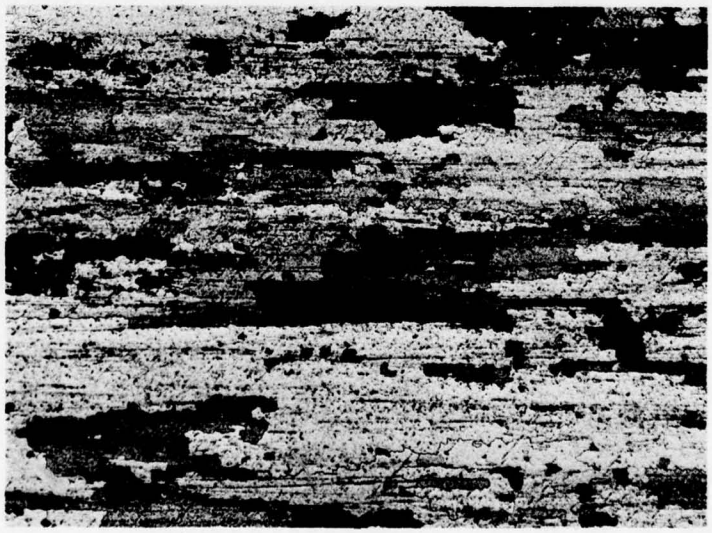

P.N. 1-50134 50X

(f) Bar V21F Extruded 1900°F (1040°C)/ 18:1/4.4 in/sec (11.2 cm/sec). Annealed 2400°F (1315°C)/1/2 hr/AC (C.E1-M.EQ.)

Figure 13 - Continued

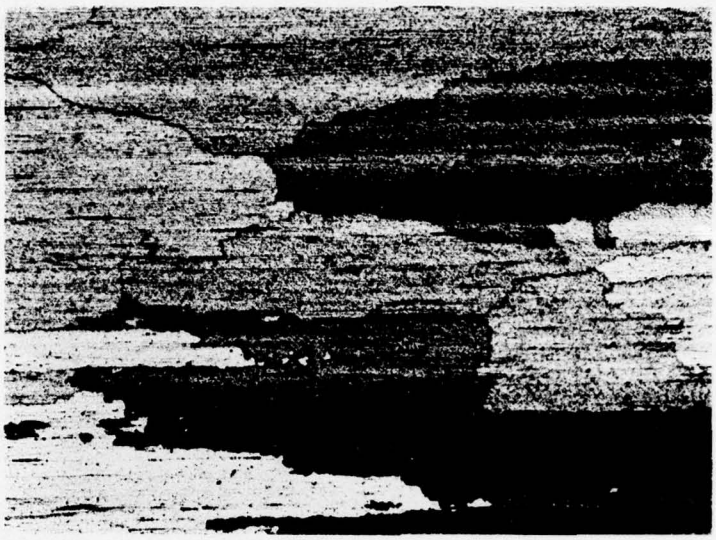

P.N. 1-50135 50X

(g) Bar V21G Extruded 2050°F (1120°C)/ 30:1/4.2 in/sec (10.7 cm/sec). Annealed 2400°F (1315°C)/1/2 hr/AC (C.EQ.)

P.N. 1-50138 50X

(h) Bar V21H Extruded 2150°F (1175°C)/ 50:1/3.2 in/sec (8.1 cm/sec). Annealed 2400°F (1315°C)/1/2 hr/AC (C.El.)

Figure 13 - Continued

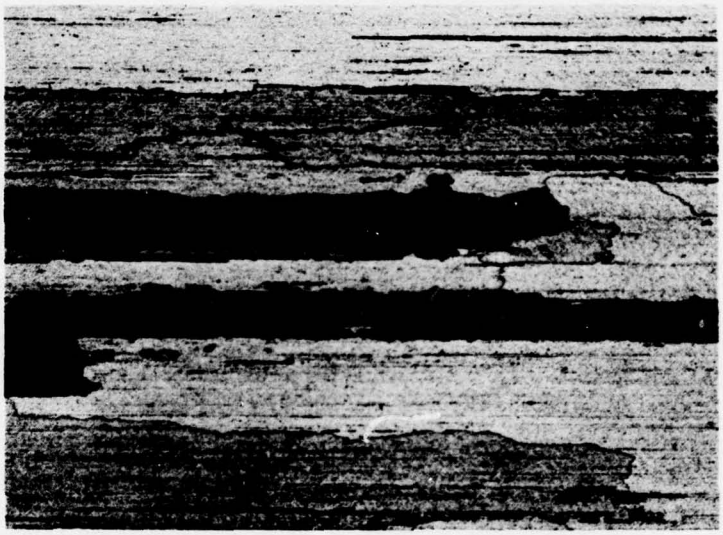

P.N. 1-50601 50X

(i) Bar V21I Extruded 2200°F (1205°C)/ 50:1/7.4 in/sec (18.8 cm/sec). Annealed 2400°F (1315°C)/1/2 hr/AC (C.El.)

Figure 13 - Continued

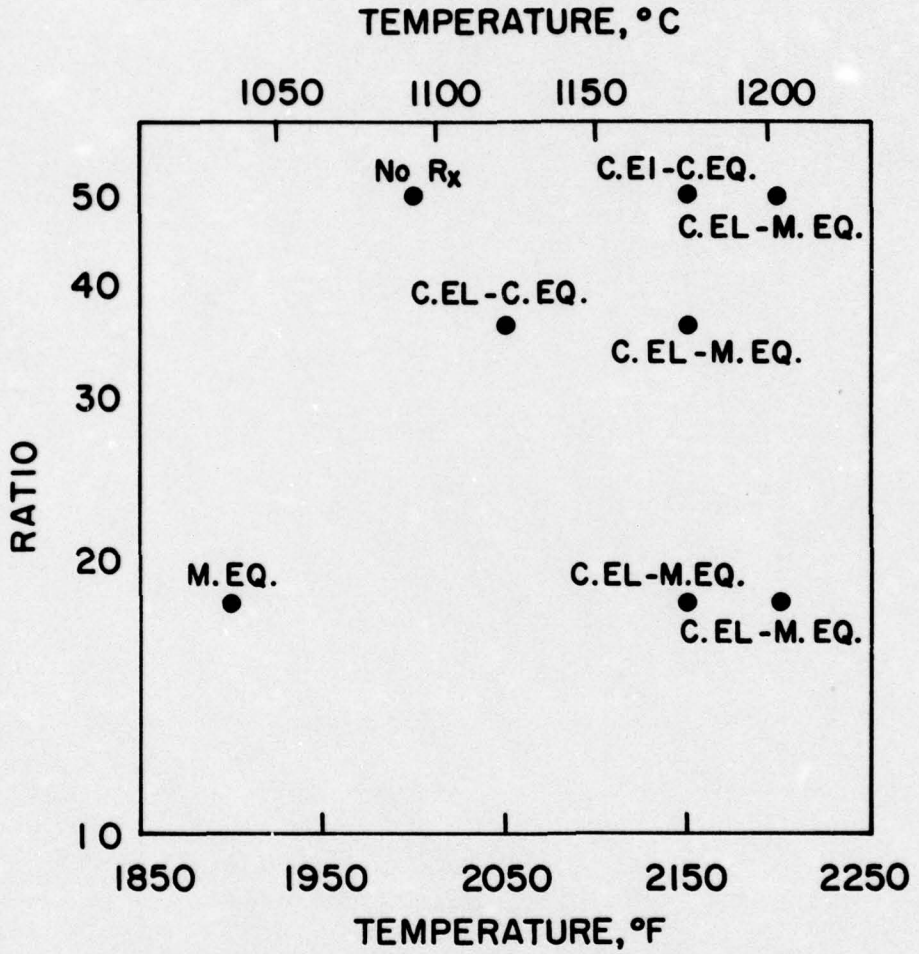

FIGURE 14 - EXTRUSION RATIO - TEMPERATURE FOR ALLOY I, V22 EXTRUSIONS SHOWING ISOTHERMAL RECRYSTALLIZATION RESPONSE.

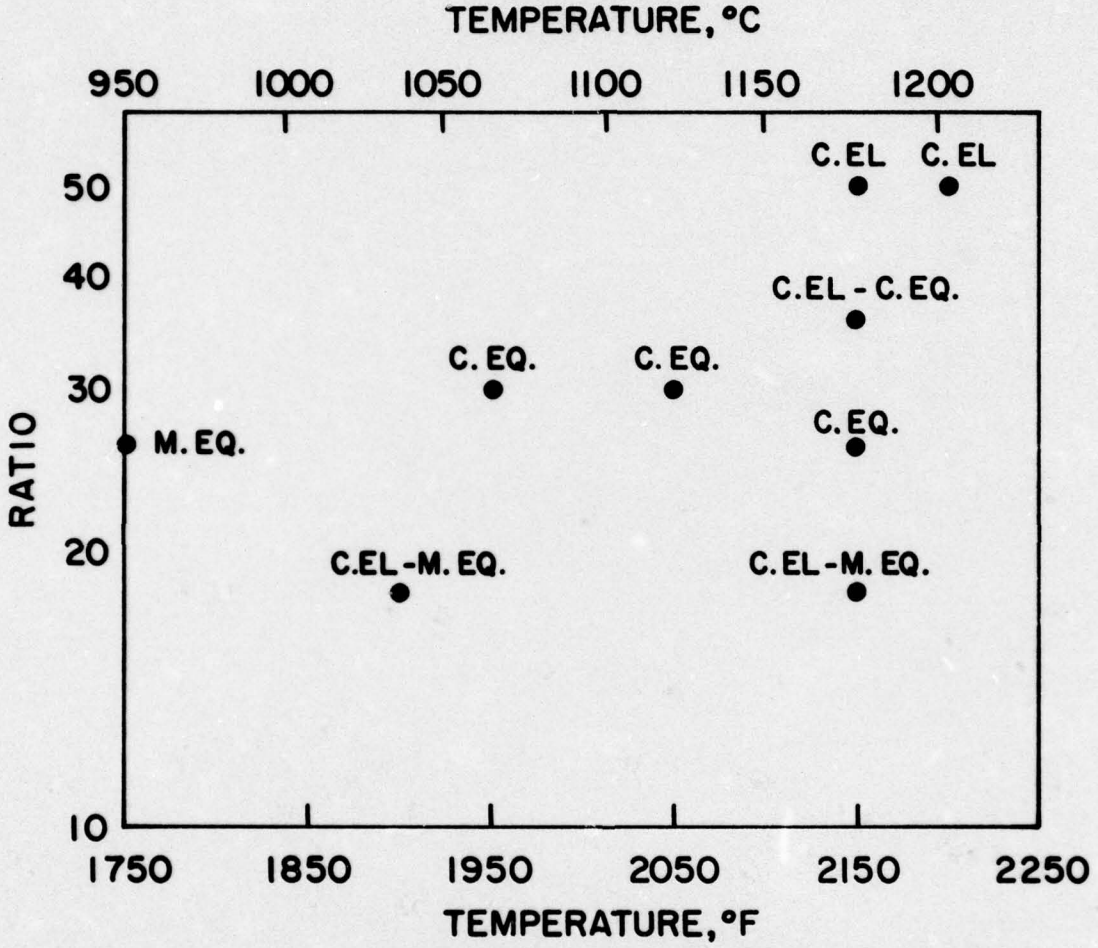

FIGURE 15 - EXTRUSION RATIO - TEMPERATURE MAP FOR ALLOY 2, V21 EXTRUSIONS SHOWING ISOTHERMAL RECRYSTALLIZATION RESPONSE.

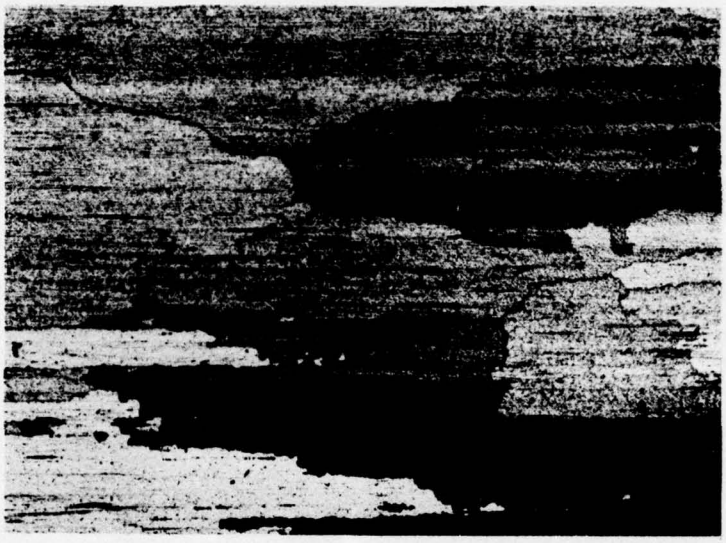

P.N. 1-50135 50X

(a) Conventional Anneal 2400°F (1315°C)/ 1/2 hr/AC. Structure: C.EQ.

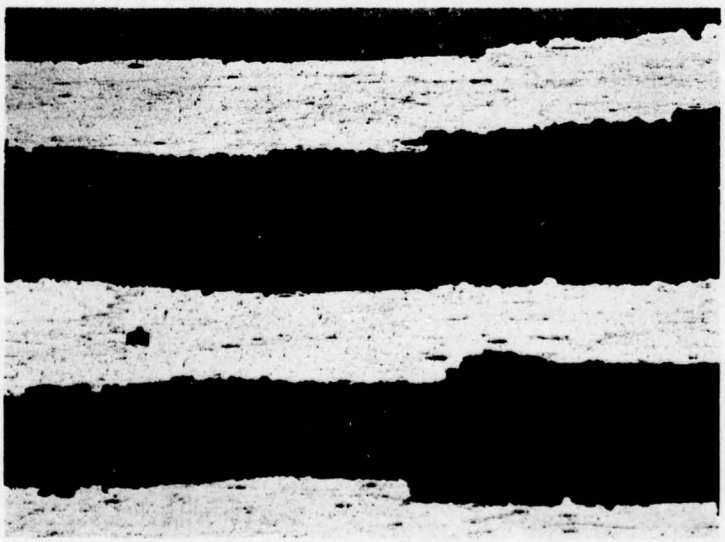

P.N. 1-50828 50X

(b) Zone Anneal 2375°F (1302°C)/5.3 iph (13.5 cmph). Structure: C.E1.

Figure 16 - Microstructures of Extruded Bar V21G, Conventional and Zone Annealed

Etchant: 45:45:10 $HCl:H_2O:H_2O_2$

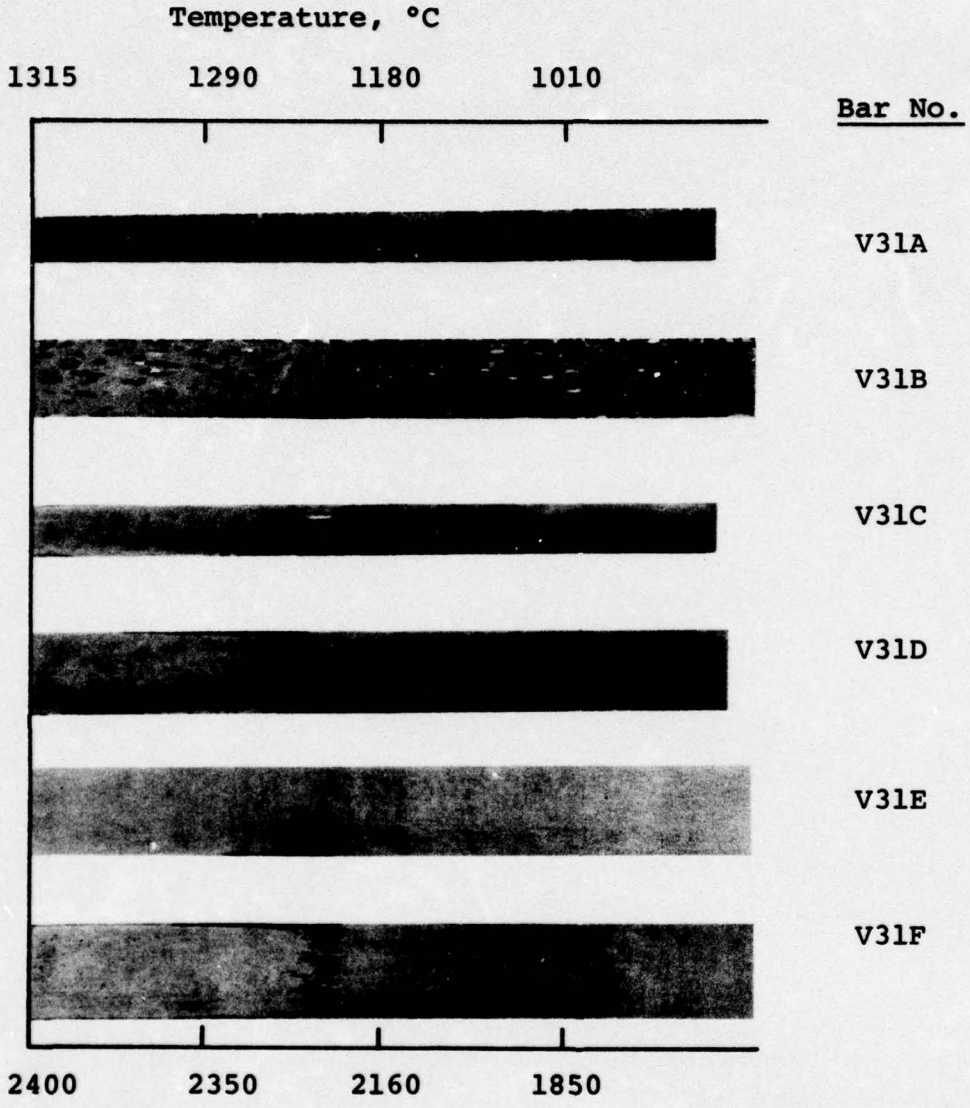

P.N.'s 2-56209, 56213, 56930 1X

Figure 17 - Macrographs of Alloy 5 Extruded and Gradient Annealed Bars

Etchant: 45:45:10 HCl:H_2O:H_2O_2

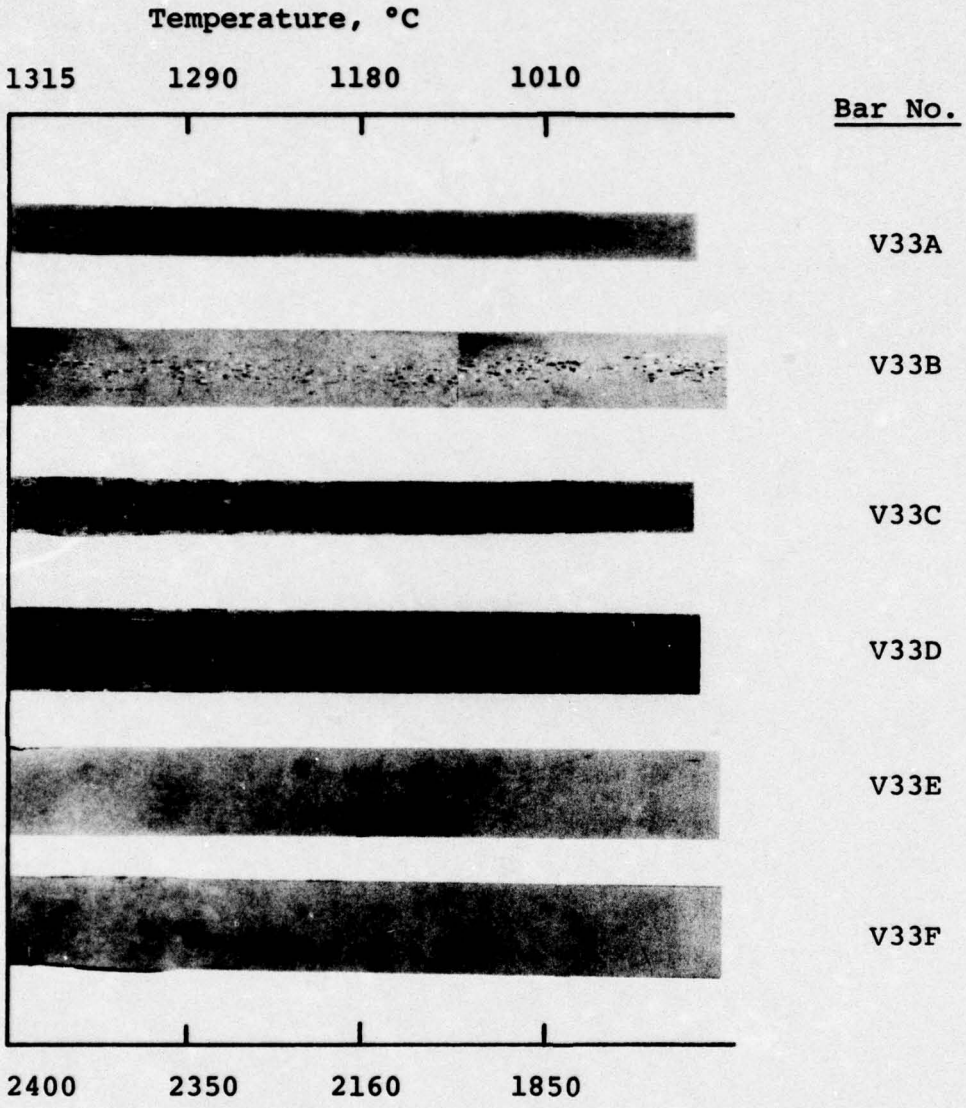

P.N.'s 2-56210, 56213, 56931 1X

Figure 18 - Macrographs of Alloy 6 Extruded and Gradient Annealed Bars

Etchant: 45:45:10 $HCl:H_2O:H_2O_2$

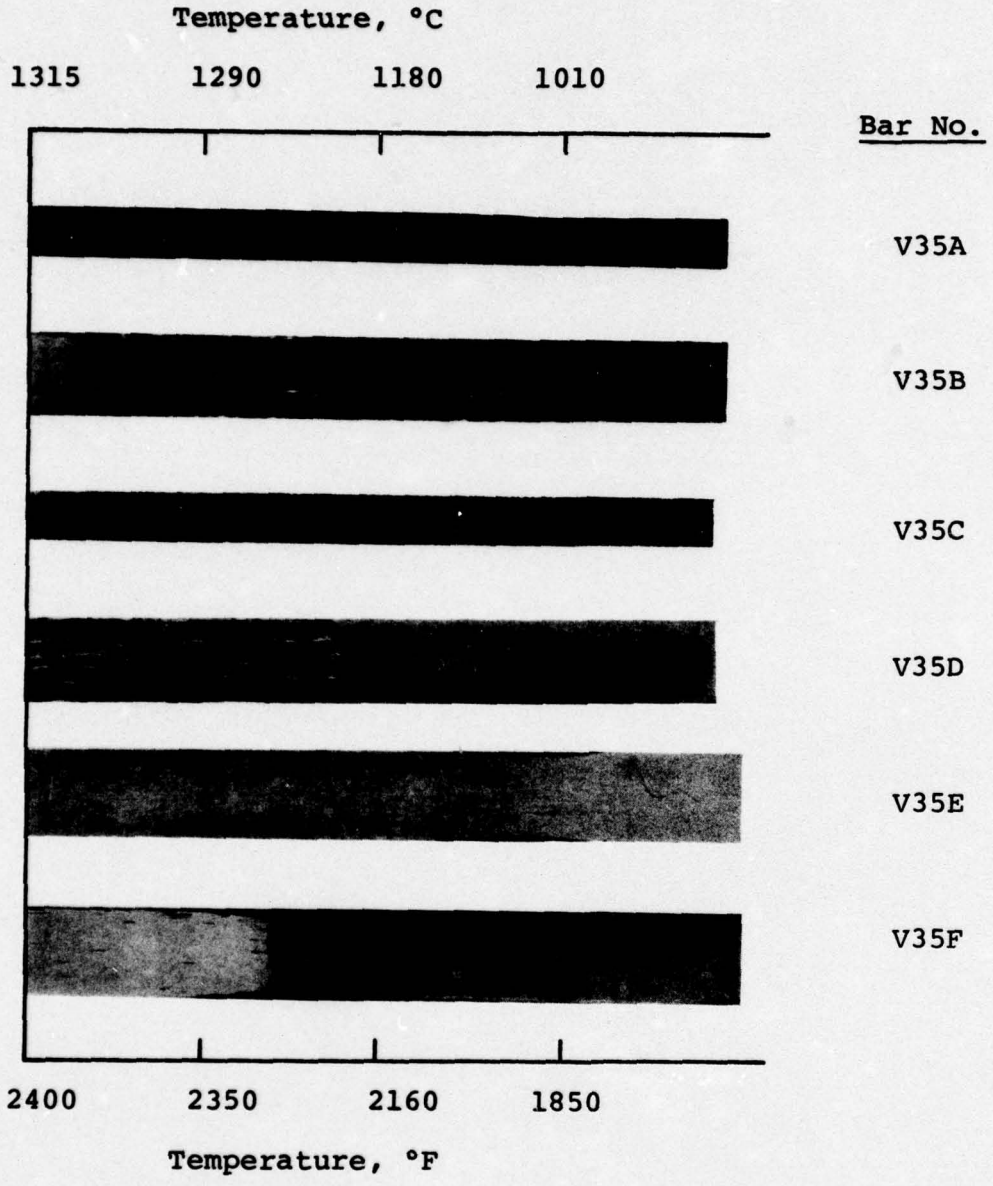

P.N.'s 2-56212, 56932 1X

Figure 19 - Macrographs of Alloy 7 Extruded and Gradient Annealed Bars

Etchant: 45:45:10 HCl:H_2O:H_2O_2

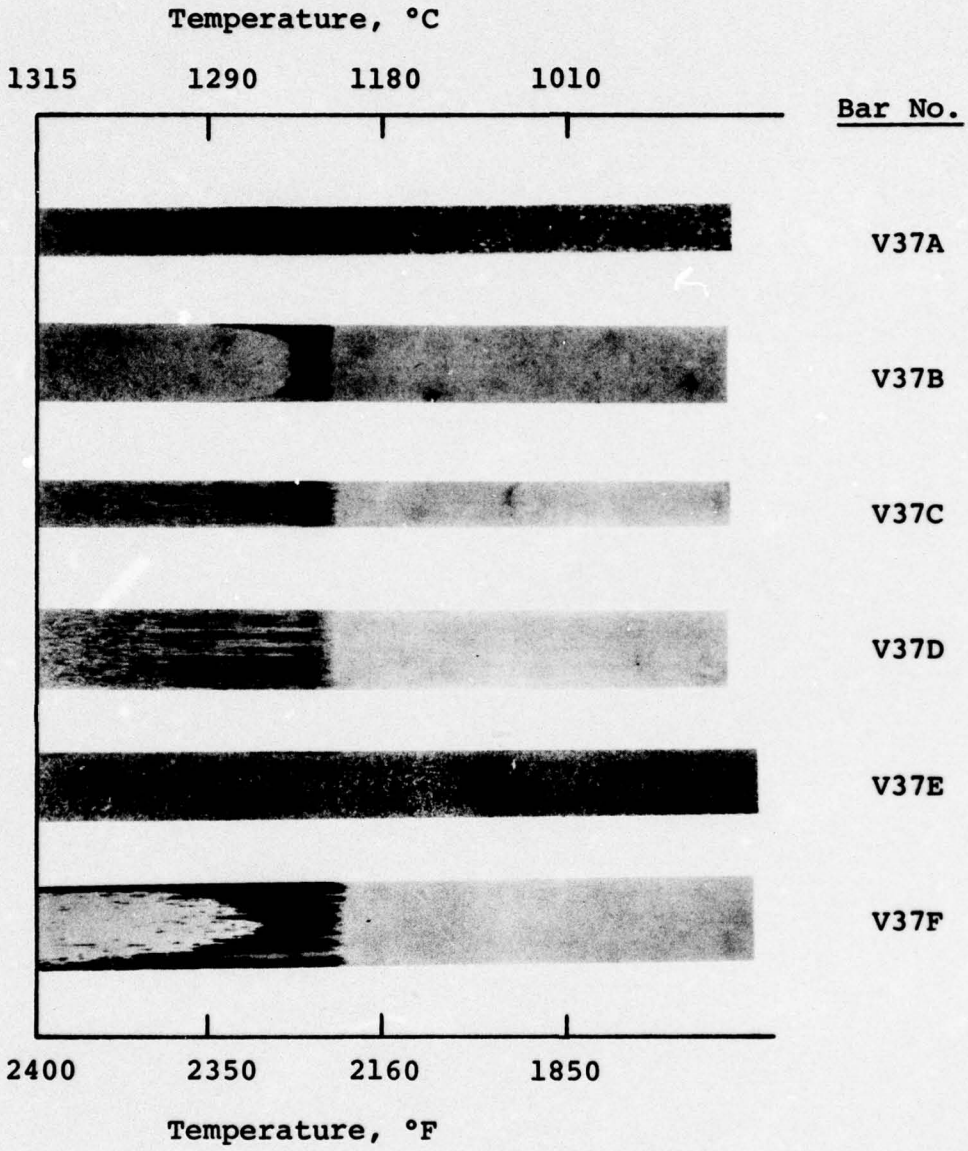

P.N.'s 2-56211, 56933 1X

Figure 20 - Macrographs of Alloy 8 Extruded and Gradient Annealed Bars

Etchant: 45:45:10 $HCl:H_2O:H_2O_2$

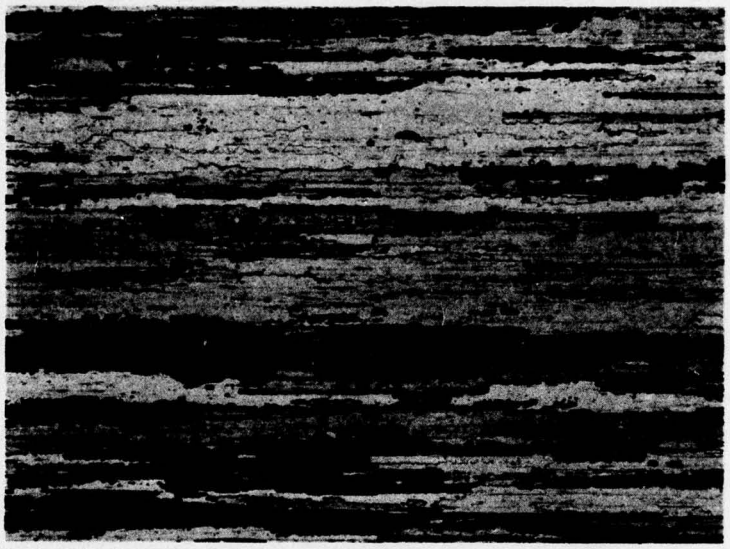

P.N. 1-57887 20X

Figure 21 - Microstructure of Zone Annealed Alloy 7, Bar V35D

Etchant: 45:45:10 $HCl:H_2O:H_2O_2$

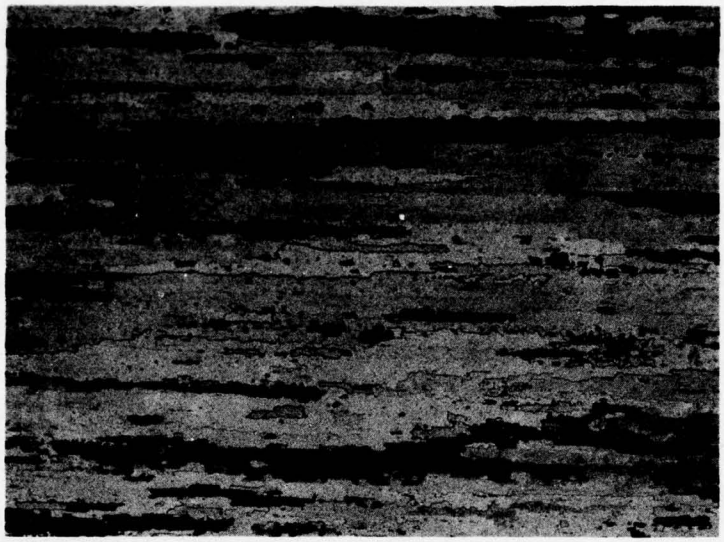

P.N. 1-57888 20X

Figure 22 - Microstructure of Zone Annealed Alloy 8, Bar V37D

Etchant: 45:45:10 $HCl:H_2O:H_2O_2$

P.N. 1-57891 20X

Figure 23 - Microstructure of Zone Annealed Alloy 8, Bar V37F

Etchant: 45:45:10 $HCl:H_2O:H_2O_2$

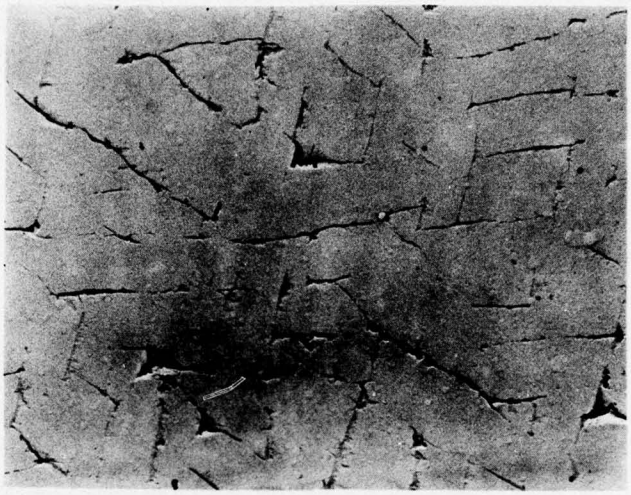

EM-018233 7800X

(a) Alloy 1 - V22B 2350°F (1290°C)/ 1/2 hr/Furnace Cool

EM-018236 7800X

(b) Alloy 2 - V21C 2350°F (1290°C)/ 1/2 hr/Furnace Cool

Figure 24 - Micrographs of γ' Size and Morphology of Alloys 1 and 2 at Near Equilibrium Conditions.

Etchant: Glyceregia

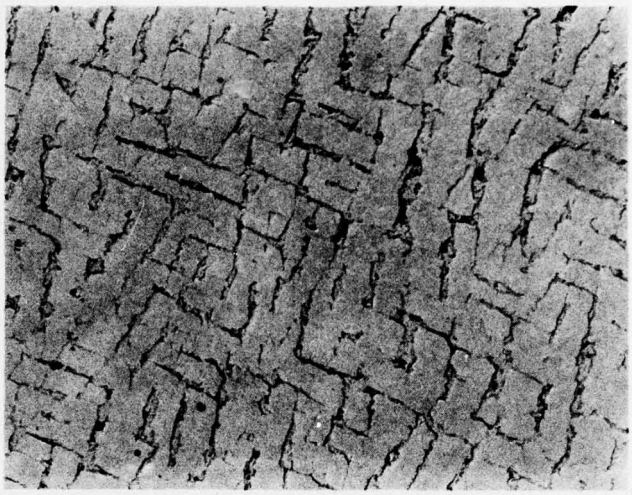

EM-018229 7800X

(a) Alloy 1 - V22B 2100°F (1150°C)/ 1/2 hr/Water Quench

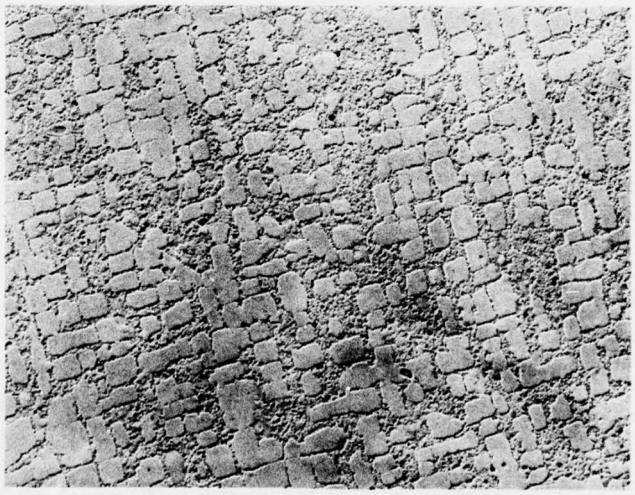

EM-018247 7800X

(b) Alloy 2 - V21C 2100°F (1150°C)/ 1/2 hr/Water Quench

Figure 25 - Micrographs of γ' Size and Morphology of Alloys 1 and 2 at 2100°F (1150°C)

Etchant: Glyceregia

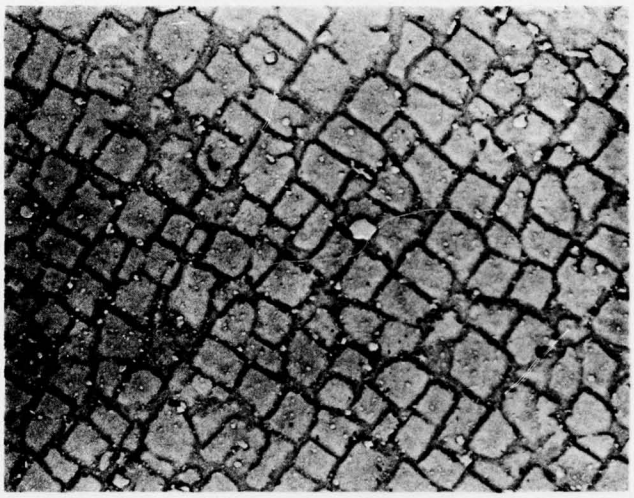

EM-019516 7800X

Figure 26 - Alloy 7 γ' Size and Morphology after Furnace Cooling from 2275°F (1247°C)

Etchant: Glyceregia

EM-019524 7800X

Figure 27 - Alloy 8 γ' Size and Morphology after Furnace Cooling from 2275°F (1247°C)

Etchant: Glyceregia

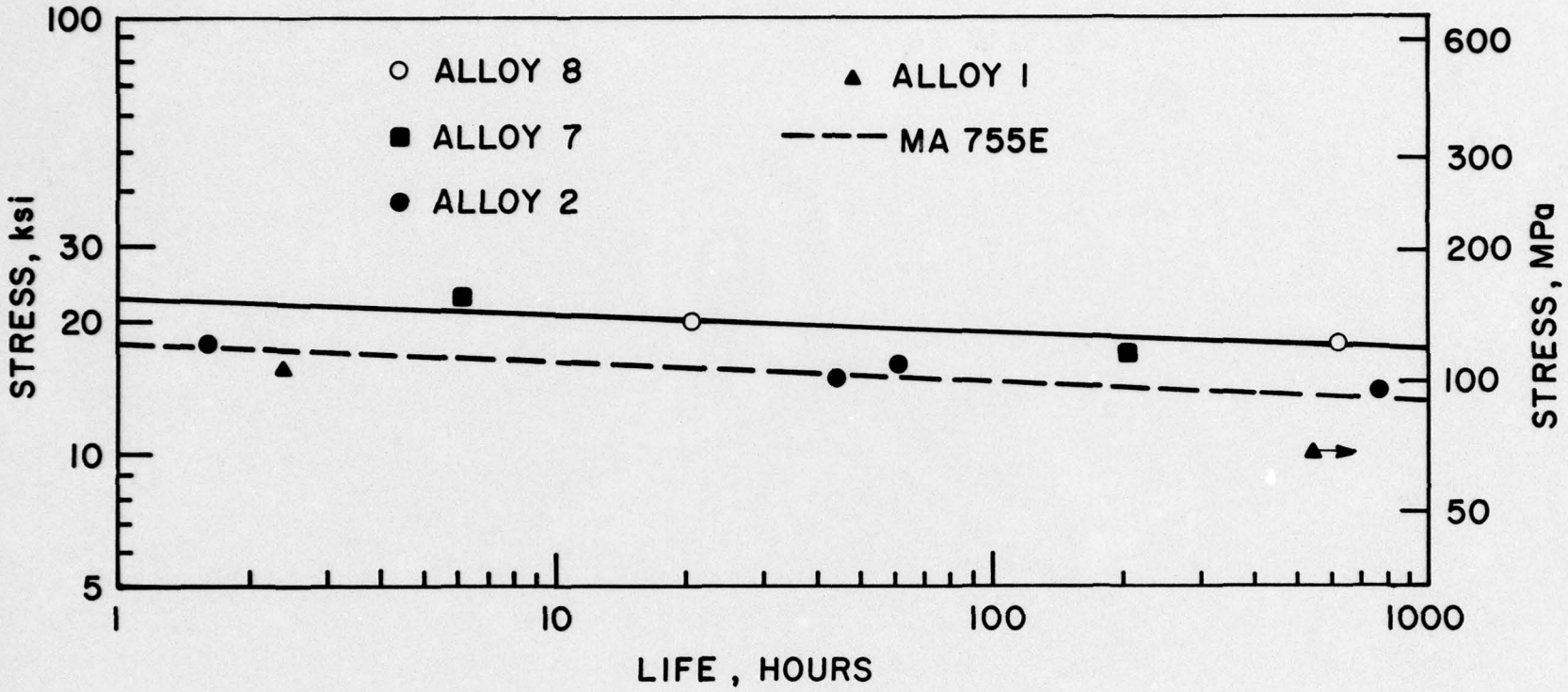

FIGURE 28 - COMPARISON OF 2000°F (1095°C) STRESS RUPTURE PROPERTIES OF ALLOYS 1, 2 , 7 AND 8 WITH MA 755E.

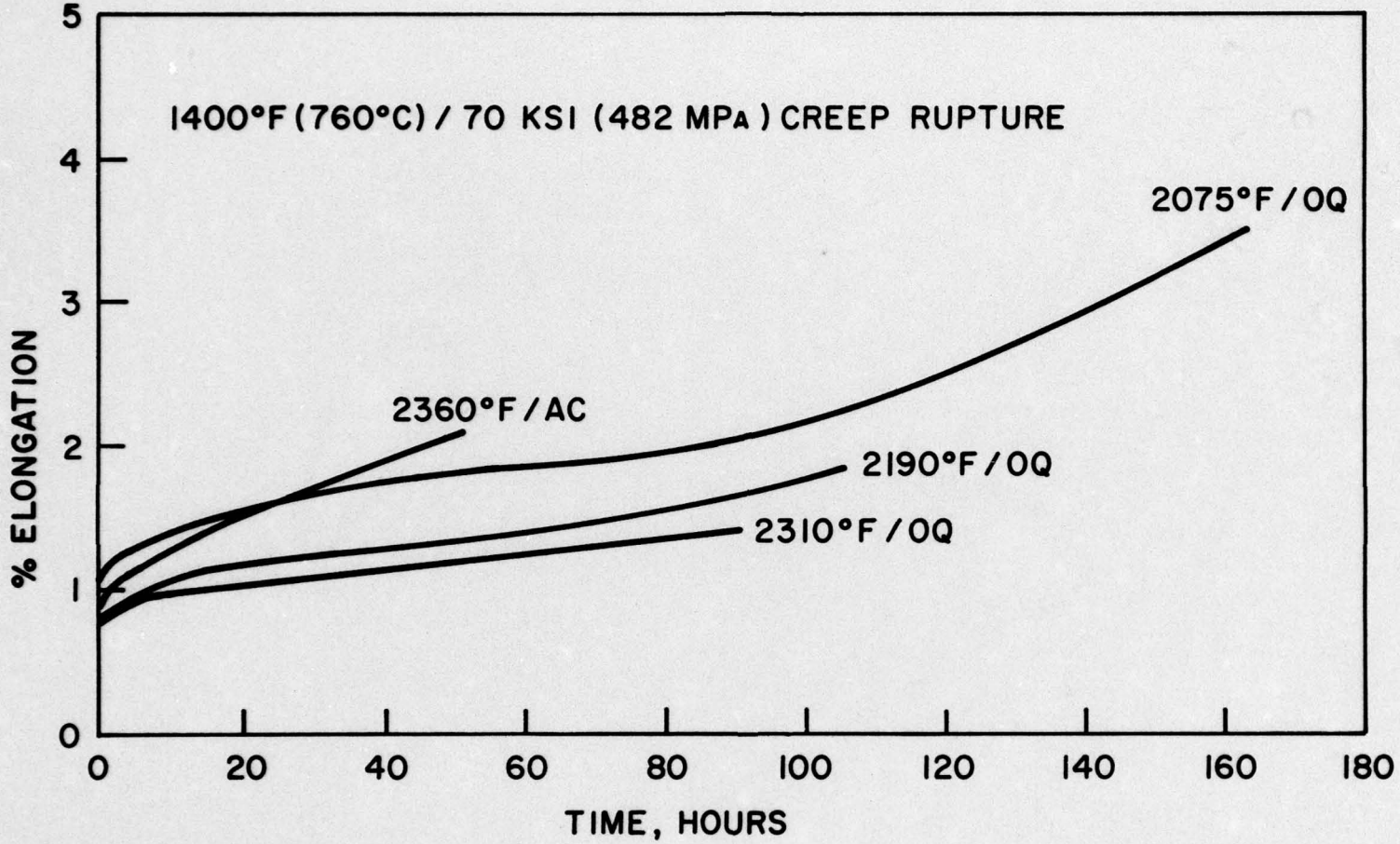

FIGURE 29 - EFFECT OF HEAT TREATMENT ON CREEP RUPTURE PLOTS FOR NAVAIR ALLOY 2.

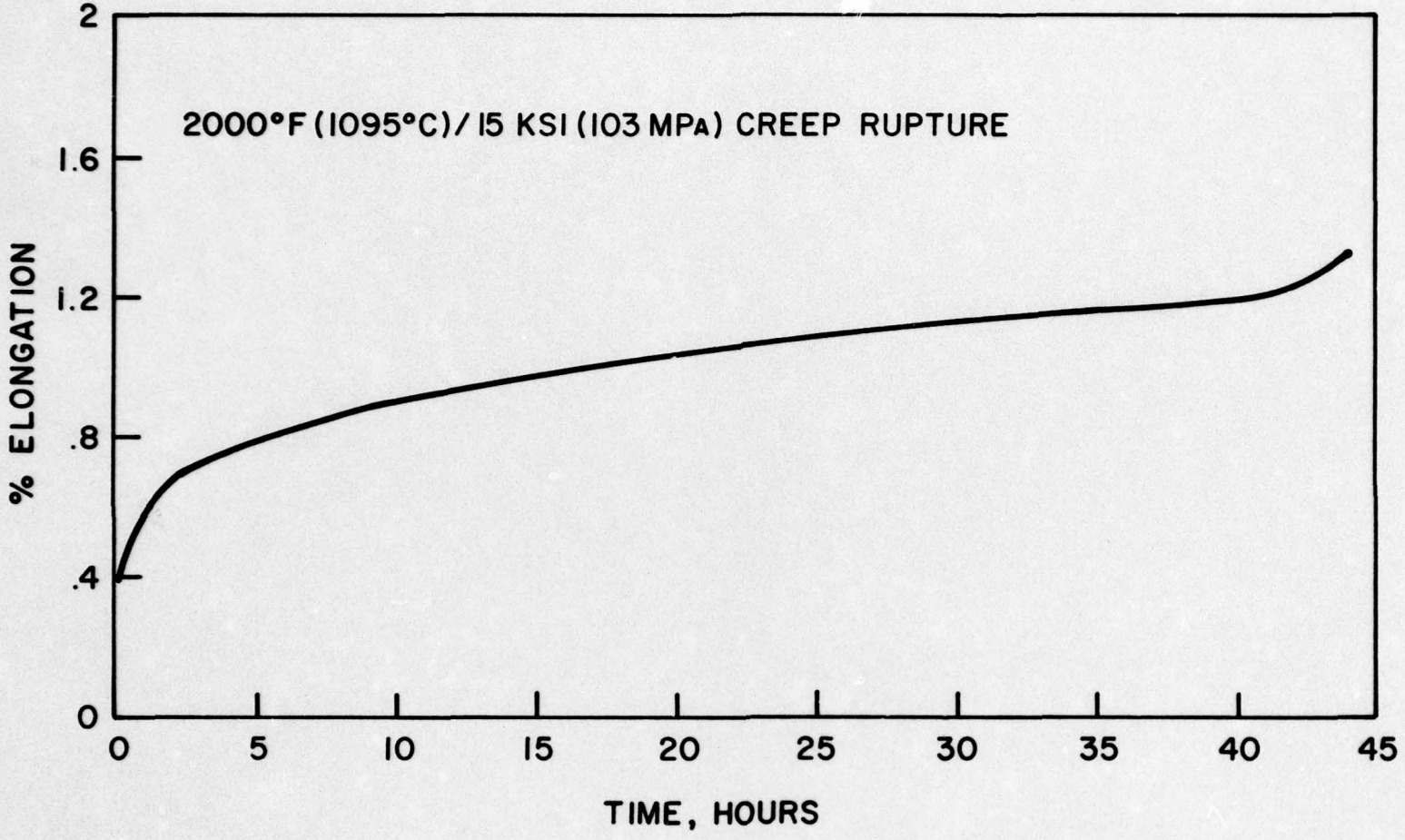

FIGURE 30 - CREEP RUPTURE PLOT FOR NAVAIR ALLOY 2.

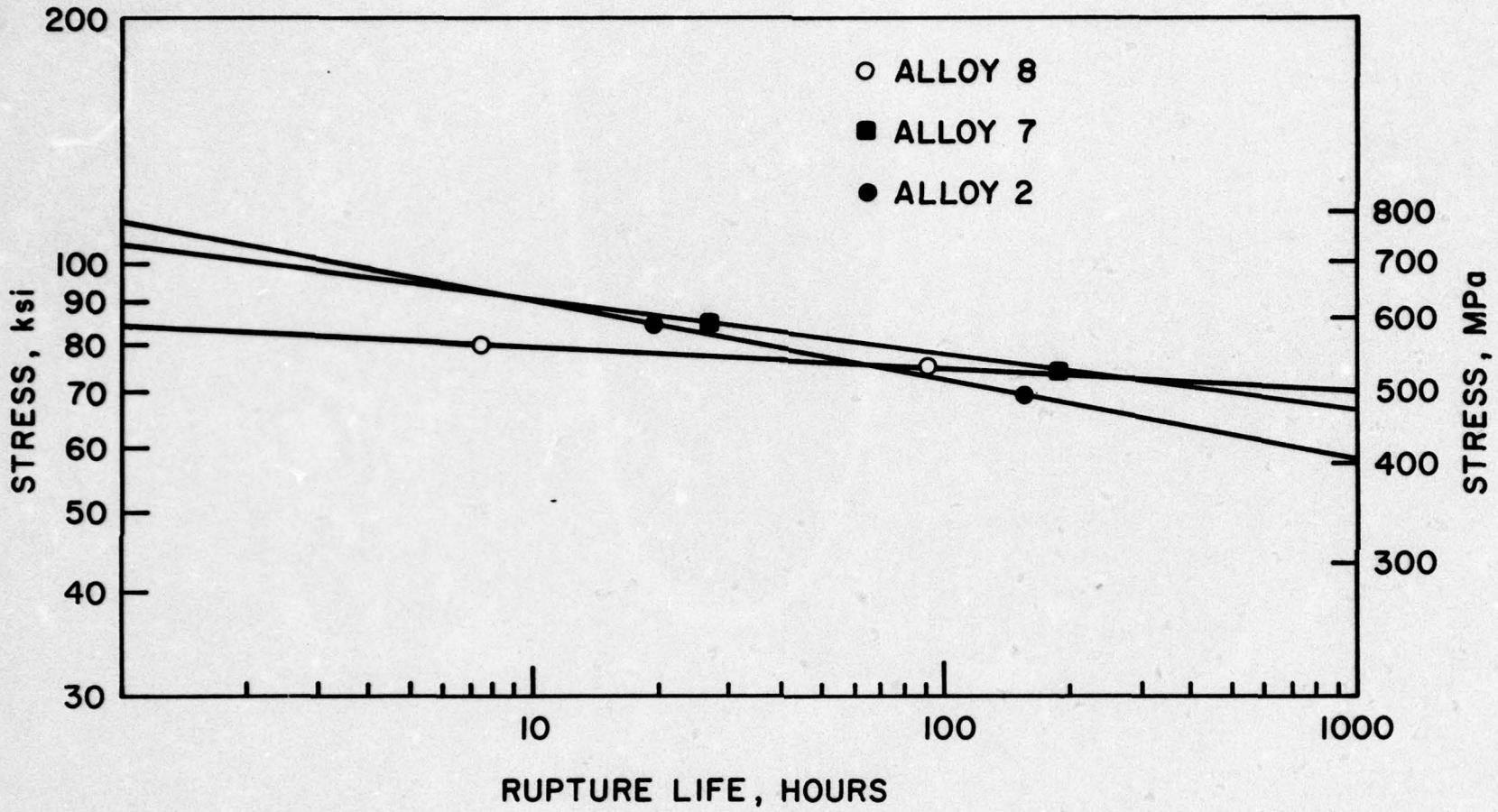

FIGURE 31 - 1400°F (760°C) STRESS RUPTURE PROPERTIES OF ALLOYS 2, 7 AND 8.

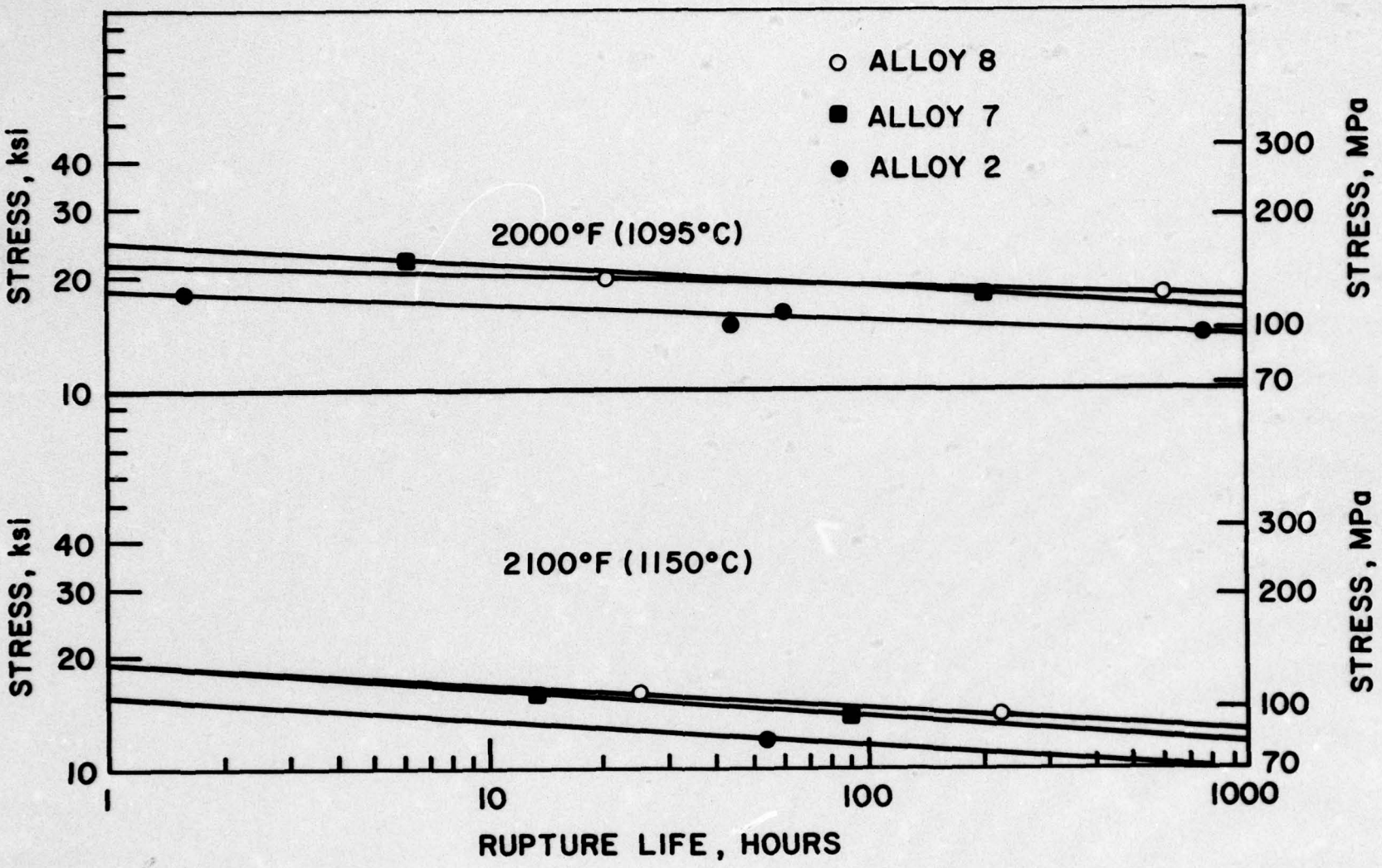

FIGURE 32 - 2000°F (1095°C) AND 2100°F (1150°C) STRESS RUPTURE PROPERTIES OF ALLOYS 2, 7 AND 8.

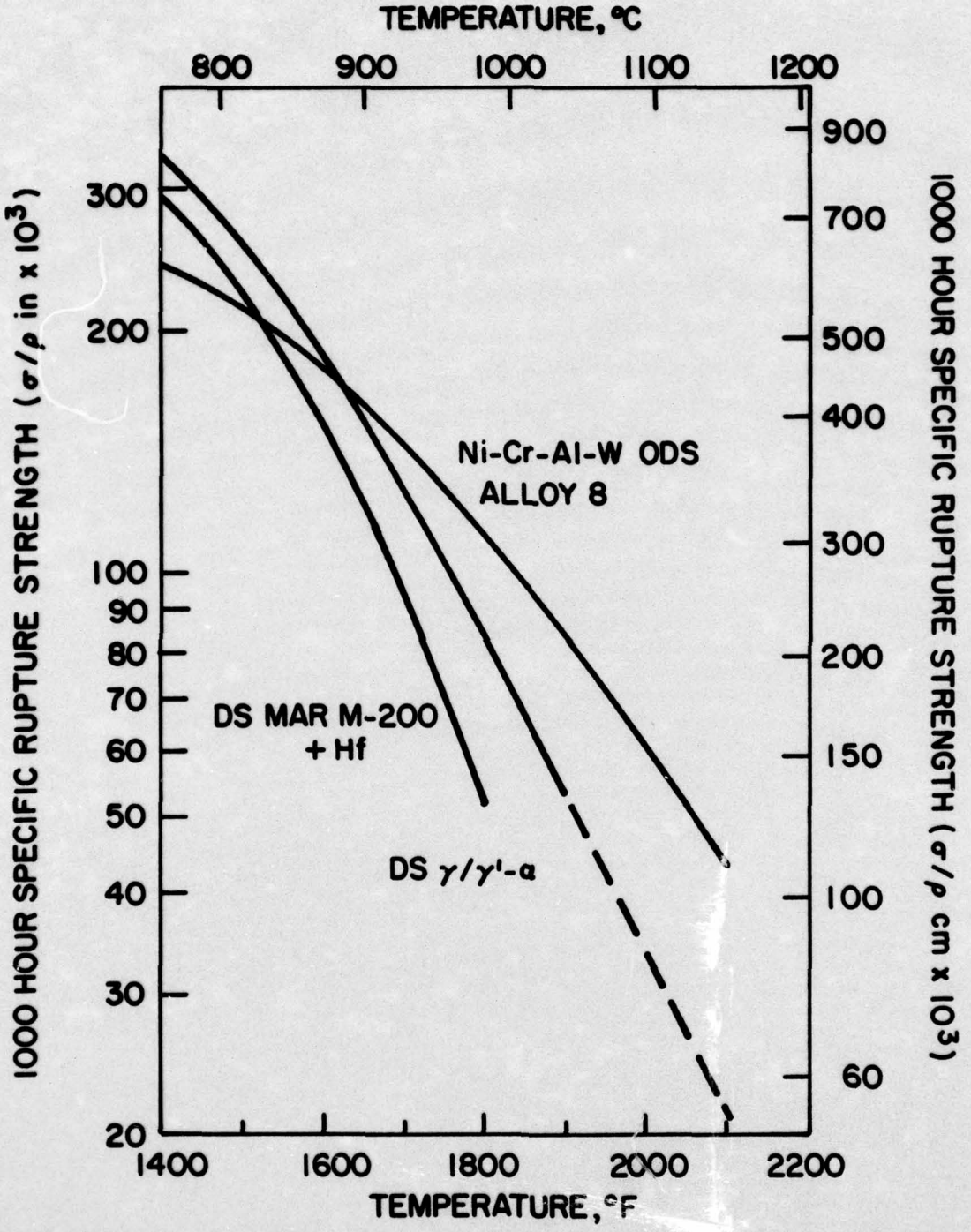

FIGURE 33 - COMPARISON OF 1000 HOUR SPECIFIC RUPTURE STRENGTH-TEMPERATURE CAPABILITY OF ALLOY 8 WITH COMPETITIVE MATERIALS.

DISTRIBUTION LIST

(one copy unless otherwise noted)

(3 copies plus balance after distribution)
U. S. Naval Air Systems Command
AIR-52031B
Department of the Navy
Washington, DC 20361

(7 copies, for internal distribution by AIR-954
AIR-954 (2 copies), AIR-536B1 (1 copy), AIR-330C (1 copy)
AIR-330E (1 copy), AIR-5361A (1 copy), AIR-5362A (1 copy)
U. S. Naval Air Systems Command
AIR- 954
Department of the Navy
Washington, DC 20361

(2 copies)
Commander
Naval Air Development Center
Code 302A, A. Fletcher (1 copy), Code 30232, E. Tankins (1 copy)
Warminster, PA 18974

(2 copies)
U. S. Naval Air Turbine Test Station
Attn: E. Lister (AT-1P) (1 copy) A. Martino (AT-1) (1 copy)
1440 Parkway Avenue
Trenton, NJ 08628

U. S. Naval Ordnance Systems Command
(ORD-33)
Department of the Navy
Washington, DC 20360

Commander
Naval Weapons Center
Code 5516
China Lake, CA 93555

(2 copies)
U. S. Naval Sea Systems Command
Code 035 (1 copy), Code 0331J (1 copy)
Department of the Navy
Washington, DC 20362

Naval Ship Engineering Center
Code 6146
Center Bldg., Room 202
Prince Georges Center
Hyattsville, MD 20782

DISTRIBUTION LIST

Naval Weapons Laboratory
Attn: W. Mannschreck
Dahlgren, VA 22448

U. S. Naval Ships Research and Development Center
Code 2812
Annapolis, MD 21402

Commander
Naval Surface Weapons Center
(Metallurgy Division)
White Oak
Silver Spring, MD 20910

(2 copies)
Director
Naval Research Laboratory
Code 6130 (1 copy)
Code 6300 (1 copy)
Washington, DC 20390

Office of Naval Research
The Metallurgy Program, Code 471
Arlington, VA 22217

Director
Army Materials and Mechanics Research Center
(A. Gorum)
Watertown, MA 02172

Commander
U. S. Armu Material Command
Attn: AMCRD-TC
5001 Eisenhower Avenue
Alexandria, VA 22304

U. S. Army Aviation Material Laboratories
Fort Eustis, VA 23604

Air Force Materials Laboratory
Code LL (1 copy)
Wright-Patterson Air Force Base
Dayton, OH 45433

Air Force Propulsion Laboratory
Code TBP
Wright-Patterson Air Force Base
OH 45433

National Aeronautics and Space Administration
Code RWM
Washington, DC 20546

DISTRIBUTION LIST

(3 copies)
National Aeronautics and Space Administration
Lewis Research Center
C. M. Ault (1 copy)
H. P. Probst (1 copy)
W. A. Sanders, MS 49-1 (1 copy)
21000 Brookpark Road
Cleveland, OH 44135

Andrew Van Echo
Energy Research & Development Administration
Division of Reactor Development and Demonstration
Mail Station F-309
Washington, DC 20545

Metals and Ceramics Information Center
Battelle Memorial Institute
505 King Avenue
Columbus, OH 43201

The Johns Hopkins University
Applied Physics Laboratory
(Maynard L. Hill)
8621 Georgia Avenue
Silver Spring, MD 20910

AVCO RAD
201 Lowell Street
Wilmington, MA 01887

ITT Research Institute
10 West 35th Street
Chicago, IL 60616

Detroit Diesel Allison Division
General Motors Corporation
Materials Laboratories
Indianapolis, IN 46206

Pratt and Whitney Aircraft
(Mr. A. Magid)
Florida Research And Development Center
West Palm Beach, FL 33402

Chief, Materials Engineering Dept.
Dept. 93-39M
Air Research Manufacturing Co. of Arizona
402 South 36th Street
Phoenix, AZ 85034

DISTRIBUTION LIST

Lycoming Division
AVCO Corporation
Stratford, CT 06497

Curtis Wright Company
Wright Aeronautical Division
Wood-Ridge, NJ 07075

Bell Aerosystems Company
Technical Library
P.O. Box 1
Buffalo, NY 14240

General Electric Company
Aircraft Engine Group
Materials and Processes Technology Laboratories
Evendale, OH 45215

Solar
(Dr. A. Metcalfe)
2200 Pacific Highway
San Diego, CA 92112

Teledyne CAE
1330 Laskey Road
Toledo, OH 43601

Stellite Division
Cabot Company
Technical Library
P.O. Box 746
Kokomo, IN 46901

(2 copies)
General Electric Co.
Corporate Research and Development
Attn: W. Hillig (1 copy)
R. Charles (1 copy)
Schenectady, NY 12301

Drexel University
College of Engineering
(Dr. A. Lawley)
Philadelphia, PA 19104

United Aircraft Research Labs
East Hartford, CT 06108

Pratt & Whitney Aircraft
Attn: Karl Winkel
East Hartford, CT 06108

DISTRIBUTION LIST

Westinghouse Electric Company
Materials and Processing Laboratory
(Ray Bratton)
Beulah Road
Pittsburg, PA 15235

Library, Research & Development Division
The Carborundum Company
P.O. Box 337
Niagara Falls, NY 14302

Ford Motor Company
Product Development Group
(E. A. Fisher)
2000 Rotunda Drive
Dearborn, MI 48121

General Electric Company
AEG Technical Information Center
Mail Drop N-32, Bldg. 700
Cincinnati, OH 45215

Professor Richard E. Tressler
Ceramic Science Section
Pennsylvania State University
201 Mineral Industries Bldg.
University Park, PA 16802

Dr. T. D. Chikalla
Ceramics and Graphite Section
Battelle - Northwest Laboratories
Richland, WA 99352

Final Report Only (12 copies for DDC)
Naval Air Systems Command
AIR- 954
Department of the Navy
Washington, DC 20361